PAPER

Permeability estimation of a porous structure in cancer treatment based on sampled velocity measurement*

To cite this article: Sepideh Afshar and Weiwei Hu 2022 Inverse Problems 38 065002

View the article online for updates and enhancements.

You may also like

- Adaptive eigenspace method for inverse scattering problems in the frequency domain

Marcus J Grote, Marie Kray and Uri Nahum

- A PDE-constrained SQP algorithm for optical tomography based on the frequency-domain equation of radiative transfer

Hyun Keol Kim and Andreas H Hielscher

- Where did the tumor start? An inverse solver with sparse localization for tumor growth models

Shashank Subramanian, Klaudius Scheufele, Miriam Mehl et al.



IOP ebooks™

Bringing together innovative digital publishing with leading authors from the global scientific community.

Start exploring the collection-download the first chapter of every title for free.

Permeability estimation of a porous structure in cancer treatment based on sampled velocity measurement*

Sepideh Afshar^{1,**} o and Weiwei Hu²

- ¹ Gordon Center for Medical Imaging, Harvard Medical School/Massachusetts General Hospital, Boston, MA 02114, United States of America
- ² Department of Mathematics, University of Georgia, Athens, GA 30602, United States of America

E-mail: safshar1@mgh.harvard.edu and Weiwei.Hu@uga.edu

Received 27 July 2021, revised 28 February 2022 Accepted for publication 23 March 2022 Published 13 April 2022



Abstract

The problem of parameter identification appears in many physical applications. A parameter of particular interest in cancer treatment is permeability, which modulates the fluidic streamlines in the tumor microenvironment. Most of the existing permeability identification techniques are invasive and not feasible to identify the permeability with minimal interference with the porous structure in their working conditions. In this paper, a theoretical framework utilizing partial differential equation (PDE)-constrained optimization strategies is established to identify a spatially distributed permeability of a porous structure from its modulated external velocity field measured around the structure. In particular, the flow around and through the porous media are governed by the steady-state Navier—Stokes—Darcy model. The performance of our approach is validated via numerical and experimental tests for the permeability of a 3D printed porous surrogate in a micro-fluidic chip based on the sampled optical velocity measurement. Both numerical and experimental results show a high precision of the permeability estimation.

Keywords: parameter identification, permeability, steady-state Navier–Stokes–Darcy model, PDE-constrained optimization, cancer treatment

(Some figures may appear in colour only in the online journal)

1361-6420/22/065002+39\$33.00 © 2022 IOP Publishing Ltd Printed in the UK

1

^{*}Submitted to the editors 26 July 2021.

^{**} Author to whom any correspondence should be addressed.

1. Introduction

In many physical applications including cancer treatment, permeability is a critical property of the structures under investigation. Some of the major fields, wherein the importance of permeability is endorsed and its estimation is well-studied, include material science [4, 10, 59], petroleum engineering [11], geoscience and reservoir engineering [3, 19, 22, 67], and tissue engineering [15, 39, 60]. However, the role of this parameter has been often overlooked in cancer treatment.

In cancer treatment, permeability is an important property of tumor tissue which modulates the interstitial flow in tumor micro-environment [57] and thus the drug delivery. In tumor tissue, the permeability is defined by cells density, alignment, and attachment [27]. Extracellular matrix (ECM) is a non-cellular component of the tumor micro-environment which plays an important role in stabilizing the spatial alignment of the cells and defines the tumor permeability [27]. The role of the tumor microenvironment and ECM in targeted drug delivery is studied in (e.g. [16, 27, 33, 57, 74, 76, 78]). Adjusting the ECM has been considered in [26, 33, 74] to enhance the drug delivery by means of weakening the ECM structure. In this regard, estimation of the permeability helps to optimize the modulation of the microenvironment towards increasing the drug transportation [27, 47, 55, 57].

In general, two different strategies have been considered in literature to estimate the permeability of a porous structure, namely, numerical and experimental approaches. Experimental estimation of the permeability is commonly used in literature. An experimental set-up is designed to characterize the pressure drop under flow dynamics through the porous structure. Estimation of the permeability is then followed by a form of Darcy's law (e.g. [37, 54, 60, 61]). Common issues with most experimental set-ups are uncertainties and constraints in sample preparation as well as complexity of the measurements. These complexities are often imposed by the assumptions required for the permeability estimation. Furthermore, the porosity of the media is assumed to be uniformly defined and distributed.

Numerical approximation of the permeability is mainly based on solving a form of flow equations over an approximate porous geometry. For this purpose, the porous structure is required to be imaged often via micro-ct/x-ray [11, 22, 29, 59] and then replaced by its void connected pathways. In most cases, the void structure is approximated by a pore-network model. The permeability is defined by estimated flow dynamics, normally in form of a capillary pressure drop, and a Darcy-like law governing the flow transport in the pore-network model [3, 11, 22, 28, 59, 73]. The efficiency and reliability of these approach depend on the imaging resolution and the pore-network approximation validity [7, 22].

In other numerical efforts to estimate the permeability, the void structure of the porous media is approximated by a simple and computationally efficient geometry over which the flow dynamics are solved on the pore scale. In one of the early works, the flow dynamics were solved over a simplified void geometry via finite element method (FEM) [75]. Later, more realistic void structures have been considered where accelerated numerical methods like lattice Boltzmann method [29, 51, 68, 71], moving particle simulation [53, 58], and even more complicated computational fluid dynamics (CFD) methods [42, 65] were proposed to define the velocity field in the porous phase and thus permeability. For structured void geometries, semi-empirical techniques, namely homogenization methods, are considered [15, 56]. Other empirical methods of permeability estimation are resorting to deep learning [31] and fractal theory coupled with microscopic Seepage flow theory [77].

The aforementioned numerical methods predominantly focus on the estimation of the void structure of the porous media. However, this information is often not provided or hard to acquire in many applications. This limitation highlights the need for a less-invasive tool to

study the flow dynamics interaction with the porous structure and estimating the permeability. The contribution of this work is twofold. First, a rigorous mathematical framework is established for the problem of distributed parameter identification of a nonlinear steady-state Navior–Stokes–Darcy model. Second, a numerical and experimental toolbox is developed for the estimation of the permeability of a tumor surrogate *in vitro*.

The parameter estimation of linear infinite-dimensional systems is well-established and reviewed in [6]. Solving the inverse problem for both linear and nonlinear PDEs with particular applications is studies in [46]. Other examples for specific classes of partial differential equations can be found in (e.g. [12, 23, 24, 30, 32, 34–36, 38, 44, 45, 49, 66]). In these studies, often, the inverse problem is solved using variational approach in which a cost function is minimized. More detailed analysis for general PDEs can be found in [25].

In general, two classes of optimization approaches for parameter estimation are often employed, namely, via stochastic optimization [62] and deterministic optimization [50] to minimize the difference between the model output and the system measurement. In this work, a deterministic optimization problem is formulated to estimate a spatially distributed permeability of a 3D porous surrogate in the continuum space. The objective is to minimize the difference between the optical measurements of the external velocity field and its corresponding flow solution of the Navier–Stokes–Darcy equations over a predefined measurement set. The optimization-based parameter estimation provides a theoretical treatment that is flexible for adjusting the microfluidic experimental design to different applications. We shall prove the existence of an optimal solution and derive the first-order optimality conditions for solving such a solution using the adjoint method.

Regarding the numerical and experimental implementation, developing an *in vitro* model for studying the properties of the tumor tissue, particularly its permeability, is a critical step toward translating new therapeutic nano-medicines into clinical application. In this work, we shall establish a noninvasive numerical and experimental framework for estimating the permeability on a microfluidic chip. The proposed approach imposes less restrictive conditions on the microenvironment of the porous surrogate to be identified compared with the proposed techniques in the literature (e.g. [17, 18, 54]). The micro-fluidic chip is designed to mimic *in vivo* conditions of the tumor environment under flow in micro-scale. Concrete examples will be presented to demonstrate our ideas and design. Our theoretical/experimental parameter estimation approach can be easily extended and adapted to different applications and potentially *in vivo* permeability identification.

2. Problem statement

This work mainly focuses on the estimation of the permeability of a porous structure from the velocity field measurement sampled around the structure. In particular, the steady-state Navier–Stokes–Darcy model is utilized to describe the flow and the porous media. The unknown parameter will be identified by minimizing the difference between the predicted velocity and its corresponding experimental measurement. To demonstrate the idea, a 2D cross section of a potential 3D microfluidic channel is shown in figure 1.

We have the following assumptions on the domain geometry for our investigation.

Assumption 2.1. Let $\Omega_f \subset \mathbb{R}^3$ be an open bounded and connected domain, with a locally Lipschitz boundary Γ_f . The boundaries Σ_w , Σ_i , Σ_o , and Σ_c are open subsets of Σ_f , which are sufficiently smooth and satisfy

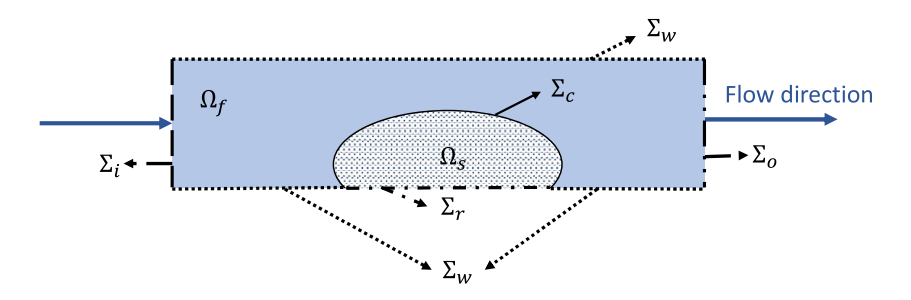


Figure 1. 2D cross section of a potential 3D microfluidic channel.

$$\begin{split} \Sigma_k \cap \Sigma_l &= \emptyset \quad \text{for} \ \ k, l \in \{\text{w}, \text{i}, \text{o}, \text{c}\}, \ k \neq l, \\ \Sigma_{\text{f}} &= \bar{\Sigma}_{\text{w}} \cup \bar{\Sigma}_{\text{i}} \cup \bar{\Sigma}_{\text{o}} \cup \bar{\Sigma}_{\text{c}}. \end{split}$$

Similarly, let $\Omega_s \subset \mathbb{R}^3$ be an open bounded and connected domain, with a locally Lipschitz boundary Γ_s . The boundary Σ_c and Σ_r are open subsets of Σ_s , which are sufficiently smooth and satisfy

$$\begin{split} \Sigma_k \cap \Sigma_l &= \emptyset \quad \text{for} \ \ k, l \in \{\text{c}, \text{r}\}, \ k \neq l, \\ \Sigma_{\text{s}} &= \bar{\Sigma}_{\text{c}} \cup \bar{\Sigma}_{\text{r}}. \end{split}$$

2.1. Steady-state Navier-Stokes-Darcy model

We consider a steady-state flow represented by the stationary Navier–Stokes equations [70]. Furthermore, the flow through the porous structure is defined by Darcy's law (e.g. [5, 8, 52]). The flow equations are solved in a channel enclosing the porous structure. The domain over which the flow dynamics is defined is divided into two sub-domains: the domain that is occupied by only the flow denoted by Ω_f and the one where both porous structure and flow are present. The domain of porous structure is denoted by Ω_s . The flow dynamics in Ω_f are defined by the pressure p and the velocity vector $u = (u_1, u_2, u_3)^T$ over $\in \Omega_f$. Let u and p denote the flow velocity and pressure around the porous structure. By mass and momentum conservation, the Navier–Stokes equations are governed by

$$\rho(u \cdot \nabla u) + \nabla p - \nabla \cdot (\mu(\nabla u + (\nabla u^{\mathsf{T}}))) = 0 \tag{2.1}$$

$$\nabla \cdot u = 0, \tag{2.2}$$

where ρ is the fluid density and μ is the fluid viscosity. The effect of the external force gravity is assumed to be negligible and, hence, neglected in our formulation. In the domain Ω_s of the porous structure, the flow equation is defined by Darcy's law and conservation of mass. Let ϕ denote the pressure along the porous structure. The flow through the porous structure is defined by (e.g. [5, 8, 52])

$$-\nabla \cdot \left(\frac{\kappa}{\mu} \nabla \phi\right) = 0, \tag{2.3}$$

where $\kappa(\cdot)$ is the permeability coefficient of the porous structure, depending on the spatial variable due to the non-homogeneous porous structure.

The boundaries consist of the boundaries of the flow domain Ω_f and the boundaries of the porous structure domain Ω_s . Note that these two domains share a boundary. The boundaries of the flow domain include the walls of the channel Σ_w , the inlet Σ_i , the outlet Σ_o , and the surface Σ_c of the porous structure which is in contact with the external flow. The boundaries of the porous structure are the contact surface Σ_c and the rest of the structure surface Σ_r .

The first part of boundary conditions are composed of no-slip condition on the surface Σ_w , a uniform known velocity profile at the flow inlet boundary Σ_i , and a uniform known pressure at the flow outlet boundary Σ_o . These conditions can be stated as

$$u = 0$$
 on $\Sigma_{\rm w}$, (2.4)

$$u = u_0$$
 on Σ_i , (2.5)

$$u \times n_0 = 0$$
 on Σ_0 , (2.6)

$$\rho \frac{|u|^2}{2} + p - n_o \cdot \mathbf{T}(u) n_o = p_0, \quad \text{on } \Sigma_o,$$
(2.7)

where $\mathbf{T}(u) = \mu(\nabla u + (\nabla u)^T)$ and n_o is the outward normal vector to the boundary Σ_o . Let $n_{\rm sf}$ be the outward normal vector to the boundary Σ_c pointing from $\Omega_{\rm s}$ to $\Omega_{\rm f}$. Then $n_{\rm fs} = -n_{\rm sf}$ stands for the outward normal vector to the boundary Σ_c pointing from $\Omega_{\rm f}$ to $\Omega_{\rm s}$. At the surface of the porous structure Σ_c , conservation of mass leads to

$$u \cdot n_{\rm sf} = q \cdot n_{\rm sf}$$
 on $\Sigma_{\rm c}$, (2.8)

where

$$q = -\frac{\kappa}{\mu} \nabla \phi \tag{2.9}$$

is the discharge velocity of the fluid relative to the solid. Similarly, balancing the normal components of the stress over the surface Σ_c results in

$$\rho \frac{|u|^2}{2} + p - n_{\rm sf} \cdot \mathbf{T}(u) n_{\rm sf} = \phi \quad \text{on } \Sigma_{\rm c}.$$
 (2.10)

The tangential component of the fluid stress is assumed to be proportional to the slip rate as described by the Beavers–Joseph–Saffman slip condition,

$$\tau \cdot \mathbf{T}(u)n_{\rm sf} = \frac{\beta\mu}{\sqrt{\kappa}}u \cdot \tau \quad \text{on } \Sigma_{\rm c}, \tag{2.11}$$

where β is the slip rate and τ is any vector linearly represented by τ_1 and τ_2 , which form a local orthonormal basis for the tangent plane to the boundary Σ_c of domain Ω_s . Finally, the flow flux on the surface Γ_r is given by

$$q \cdot n_{\rm r} = q_0(x)$$
 on $\Sigma_{\rm r}$, (2.12)

where $n_{\rm r}$ is the outward normal vector to the boundary $\Sigma_{\rm r}$ of domain $\Omega_{\rm s}$.

Let P_{τ} be the projection onto the local tangential plane that can be explicitly defined as

$$P_{\tau}u = \sum_{i=1}^{2} (u \cdot \tau_i)\tau_i = u - (u \cdot n_{\rm sf})n_{\rm sf} = u - (u \cdot n_{\rm fs})n_{\rm fs}. \tag{2.13}$$

2.2. The problem of permeability identification

As mentioned earlier, the objective of the current work is to identify the unknown permeability $\kappa(\cdot)$ based on the sampled data from the velocity field measurements. Consider that the velocity measurements are taken as the local measurements over subdomains Ω_i , $i = 1, 2, \dots, m$, of the flow domain Ω_f , centered at some point $\xi_i \in \Omega_f$ with radius $\epsilon_i > 0$. Let $\vec{y} = [y_1, y_2, \dots, y_m]^T \in$ \mathbb{R}^m denote the experimental samples of the velocity field measurements, $\mathcal{X} = (L^2(\Omega_{\mathrm{f}}))^3$, and $\mathcal{Y} = \mathbb{R}^m$ be the output measurement space. Define the output measurement operator \mathcal{C} : $\mathcal{X} \to \mathcal{Y}$ by

$$\vec{y} = Cu = \left[\int_{\Omega_{f}} c_{\Omega_{1}}(x)u \, dx, \int_{\Omega_{f}} c_{\Omega_{2}}(x)u \, dx, \dots, \int_{\Omega_{f}} c_{\Omega_{m}}(x)u \, dx \right]^{T}, \quad \forall \ u \in \mathcal{X},$$

$$(2.14)$$

where $c_{\Omega_i}(\cdot)$ is defined by

$$c_{\Omega_i}(x) = \begin{cases} \frac{1}{\epsilon_i} & \text{if } |x - \xi_i| \leqslant \epsilon_i, \\ 0 & \text{otherwise.} \end{cases}$$
 (2.15)

In other words, $y_i = \frac{1}{\epsilon_i} \int_{\Omega_i} u \, dx$, i = 1, 2, ..., m. We formulate the parameter identification problem as the following minimization problem

$$J(\kappa) = \frac{1}{2} \|\mathcal{C}u - \vec{y}_{\text{ref}}\|_{\mathcal{Y}}^2 + \frac{\alpha}{2} \|\kappa\|_{\mathbb{K}}^2, \qquad (P)$$

subject to (2.1)–(2.12), for some weight parameter $\alpha > 0$, where $\vec{y}_{ref} \in \mathbb{R}^m$ is a given reference velocity vector and \mathbb{K} stands for the set of admissible functions for $\kappa(\cdot)$. Since the output measurement usually involves noises, to unify the optimal solution we consider a regularized optimization criterion defined as the Tikhonov functional. The choice of $\mathbb K$ is tied to the physical properties as well as the need to establish the existence of an optimal solution and the first-order optimality conditions for solving such a solution. Since $\kappa(\cdot)$ is the coefficient of ∇p and $\nabla \phi$, which also appears in the interface condition (2.11), the mapping $\kappa \mapsto u$ is nonlinear. As a result, problem (P) becomes non-convex. In fact, the nonlinearity of the Navier-Stokes equations has been shown to disturb the convexity (e.g. [1], p 307), let along the nonlinear coupling of these equations with Darcy's law. Therefore, the uniqueness of the optimal solution may not hold in general. Moreover, to establish the optimality conditions, mathematically, it is critical to identify the appropriate regularity for \mathbb{K} as to allow the differentiability of the mapping $\kappa \mapsto u$. Since the tumor tissue is not experiencing sharp variation, it is reasonable to assume that the permeability is sufficiently regular.

The remainder of this paper is organized as follows. The weak formulation and wellposedness of the system model are addressed in section 3. A rigorous proof of the existence of an optimal solution is presented in section 4. The first-order optimality conditions for characterizing and solving the optimal solution are established in section 5 using the adjoint method. Finally, the numerical and experimental test results are demonstrated in section 6. This work is concluded in section 7.

In the sequel, the symbol C denotes a generic positive constant, which is allowed to depend on the domain as well as on indicated parameters without ambiguity.

3. Weak formulation of the system model

For the convenience of our discussion, we define the affine space

$$V_{u_0}^1(\Omega_f) = \{ u \in (H^1(\Omega_f))^3 : \text{div } u = 0, \ u|_{\Sigma_w} = 0, \ u|_{\Sigma_i} = u_0, \text{ and } u \times n|_{\Sigma_0} = 0 \},$$

and the function spaces

$$V_0^1(\Omega_{\rm f}) = \{u \in (H^1(\Omega_{\rm f}))^3 : \text{div } u = 0, \ u|_{\Sigma_{\rm w} \cup \Sigma_{\rm i}} = 0, \text{ and } u \times n_{\rm o}|_{\Sigma_{\rm o}} = 0\},$$

$$V = V_0^1(\Omega_{\rm f}) \times H^1(\Omega_{\rm s}),$$

$$H = (L^2(\Omega_{\rm f}))^3 \times L^2(\Omega_{\rm s}).$$

Moreover, let

$$\mathbb{K} = \{ \kappa \in H^1(\Omega_s) : 0 < \kappa_l \le \kappa \le \kappa_u < \infty, \text{ a.e. } x \in \Omega_s \},$$

where k_l and k_u are positive constants. Let $(\cdot, \cdot)_D$ denote the L^2 -inner product on the domain D $(D = \Omega_f \text{ or } \Omega_s)$ and $\langle \cdot, \cdot \rangle$ denote the L^2 -inner product on the domain boundary or the duality paring between the Banach space X and its dual space X^* .

To define the weak solution of the coupled Navier–Stokes–Darcy problem (2.1)–(2.12), we first introduce the associated bilinear and trilinear forms.

For the Navier–Stokes equations (2.1) over Ω_f , taking the inner product of its linear part with $w \in V_0^1(\Omega_f)$ and using the boundary conditions (2.4)–(2.11) we obtain

$$\begin{split} &\left(-\nabla\cdot\left(\mu(\nabla u+(\nabla u)^{\mathrm{T}})+\nabla p,w\right)_{\Omega_{\mathrm{f}}}\right) \\ &=\frac{1}{2\mu}\int_{\Omega_{\mathrm{f}}}\mathbf{T}(u)\cdot\mathbf{T}(w)\mathrm{d}x-\int_{\Sigma_{\mathrm{o}}\cup\Sigma_{\mathrm{c}}}(\mathbf{T}(u)n)\cdot w\,\mathrm{d}x+\int_{\Sigma_{\mathrm{o}}\cup\Sigma_{\mathrm{c}}}p(w\cdot n)\mathrm{d}x \\ &=\frac{1}{2\mu}\int_{\Omega_{\mathrm{f}}}\mathbf{T}(u)\cdot\mathbf{T}(w)\mathrm{d}x-\int_{\Sigma_{\mathrm{c}}}(\mathbf{T}(u)n_{\mathrm{fs}})\cdot\left[(w\cdot n_{\mathrm{fs}})n_{\mathrm{fs}}+P_{\tau}w\right]\mathrm{d}x \\ &-\int_{\Sigma_{\mathrm{o}}}(\mathbf{T}(u)n_{\mathrm{o}})\cdot w\,\mathrm{d}x+\int_{\Sigma_{\mathrm{c}}}(pn_{\mathrm{fs}})\cdot\left[(w\cdot n_{\mathrm{fs}})n_{\mathrm{fs}}+P_{\tau}w\right]\mathrm{d}x+\int_{\Sigma_{\mathrm{o}}}p(w\cdot n_{\mathrm{o}})\mathrm{d}x \\ &=\frac{1}{2\mu}\int_{\Omega_{\mathrm{f}}}\mathbf{T}(u)\cdot\mathbf{T}(w)\mathrm{d}x+\int_{\Sigma_{\mathrm{c}}}\phi(w\cdot n_{\mathrm{fs}})\mathrm{d}x-\frac{\rho}{2}\int_{\Sigma_{\mathrm{c}}}|u|^{2}(w\cdot n_{\mathrm{fs}})\mathrm{d}x \\ &+\int_{\Sigma_{\mathrm{c}}}\frac{\beta\mu}{\sqrt{\kappa}}(P_{\tau}u)\cdot(P_{\tau}w)\mathrm{d}x+\int_{\Sigma_{\mathrm{o}}}p_{\mathrm{o}}(w\cdot n_{\mathrm{o}})\mathrm{d}x-\frac{\rho}{2}\int_{\Sigma_{\mathrm{o}}}|u|^{2}(w\cdot n_{\mathrm{o}})\mathrm{d}x, \end{split}$$

where $n|_{\Sigma_0} = n_0$ and $n|_{\Sigma_c} = n_{\rm fs}$. Now define the bilinear form $a_{\rm f}(\cdot,\cdot): V_0^1(\Omega_{\rm f}) \times V_0^1(\Omega_{\rm f}) \to \mathbb{R}$ by

$$a_{f}(u,w) = \frac{1}{2\mu} \int_{\Omega_{f}} \mathbf{T}(u) \cdot \mathbf{T}(w) dx + \int_{\Sigma_{c}} \phi(w \cdot n_{fs}) dx + \int_{\Sigma_{c}} \frac{\beta \mu}{\sqrt{\kappa}} (P_{\tau}u) \cdot (P_{\tau}w) dx + \int_{\Sigma_{o}} p_{0}(w \cdot n_{o}) dx - \frac{\rho}{2} \int_{\Sigma_{o} \cup \Sigma_{c}} |u|^{2} (w \cdot n) dx.$$
(3.1)

Next define the trilinear form $b(\cdot,\cdot,\cdot):V^1_0(\Omega_{\mathrm{f}})\times V^1_0(\Omega_{\mathrm{f}})\times V^1_0(\Omega_{\mathrm{f}})\to \mathbb{R}$. Note that

$$u \cdot \nabla u = \omega \times u + \frac{1}{2} \nabla |u|^2, \quad \omega = \nabla \times v.$$

For $w \in V_0^1(\Omega_f)$, we have

$$b(u, u, w) = (\rho(u \cdot \nabla u), w)_{\Omega_{f}} = \rho((\nabla \times u) \times u), w)_{\Omega_{f}} + \rho\left(\frac{1}{2}\nabla|u|^{2}, w\right)_{\Omega_{f}}$$
$$= \rho((\nabla \times u) \times u), w)_{\Omega_{f}} + \frac{\rho}{2} \int_{\Sigma_{0} \cup \Sigma_{c}} |u|^{2} (w \cdot n) dx. \tag{3.2}$$

For the porous media over Ω_s , the bilinear form $a_s(\cdot,\cdot):H^1(\Omega_f)\times H^1(\Omega_f)\to \mathbb{R}$ is defined by

$$a_{s}(\phi, \psi) = -\left\langle \frac{\kappa}{\mu} \nabla \phi \cdot n, \psi \right\rangle_{\Sigma_{c} \cup \Sigma_{r}} + \left(\frac{\kappa}{\mu} \nabla \phi, \nabla \psi \right)_{\Omega_{s}}$$

$$= \langle u \cdot n_{sf}, \psi \rangle_{\Sigma_{c}} + \langle q_{0}, \psi \rangle_{\Sigma_{r}} + \left(\frac{\kappa}{\mu} \nabla \phi, \nabla \psi \right)_{\Omega_{s}}.$$
(3.3)

Given (3.1)-(3.3), the weak formulation of the governing system (2.1)-(2.12) is then defined as follows: find $(u, \phi) \in V^1_{u_0}(\Omega_f) \times H^1(\Omega_s)$ such that

$$\bar{a}((u,\phi);(w,\psi)) + \bar{b}(u,u,w) = L(w,\psi), \quad \forall \ (w,\psi) \in V, \tag{3.4}$$

where

$$\bar{a}((u,\phi);(w,\psi)) = \frac{1}{2\mu} \int_{\Omega_{\rm f}} \mathbf{T}(u) \cdot \mathbf{T}(w) dx + \int_{\Sigma_{\rm c}} \phi(w \cdot n_{\rm fs}) dx + \int_{\Sigma_{\rm c}} \frac{\beta \mu}{\sqrt{\kappa}} \times (P_{\tau}u) \cdot (P_{\tau}w) dx,
+ \int_{\Sigma_{\rm c}} (u \cdot n_{\rm sf}) \psi \, dx + \int_{\Omega_{\rm c}} \frac{\kappa}{\mu} \nabla \phi \cdot \nabla \psi \, dx,$$
(3.5)

for $\forall (u, \phi), (w, \psi) \in (H^1(\Omega_f))^3 \times H^1(\Omega_s)$,

$$\bar{b}(u, v, w) = \int_{\Omega_{f}} \rho((\nabla \times u) \times v) \cdot w \, dx, \quad \forall \ u, v, w \in (H^{1}(\Omega_{f}))^{3}$$
 (3.6)

$$L(w,\psi) = \int_{\Sigma_{o}} p_{0}(w \cdot n_{o}) dx + \int_{\Sigma_{r}} q_{0}\psi dx, \quad \forall \ w \in (H^{1}(\Omega_{f}))^{3}, \psi \in H^{1}(\Omega_{s}).$$
(3.7)

(3.7)

Lemma 3.1. *The bilinear form* $\bar{a}(\cdot,\cdot): V \times V \to \mathbb{R}$ *is continuous and coercive.*

Proof. (Please refer to appendix A.)

Furthermore, for the trilinear form $b(\cdot, \cdot, \cdot)$ we have for $u, v, w \in (H^1(\Omega_f))^3$,

$$\bar{b}(u, v, w) = \int_{\Omega_{f}} \rho((\nabla \times u) \times v) \cdot w \, dx$$

$$\leq \rho \|\nabla u\|_{L^{2}(\Omega_{f})} \|v\|_{L^{4}(\Omega_{f})} \|w\|_{L^{4}(\Omega_{f})}$$

$$\leq C_{\bar{b}} \rho \|u\|_{H^{1}(\Omega_{f})} \|v\|_{H^{1}(\Omega_{f})} \|w\|_{H^{1}(\Omega_{f})}, \tag{3.8}$$

for some $C_{\bar{b}} > 0$ depending only on $\Omega_{\rm f}$. In particular, since $((\nabla \times u) \times v) \cdot v = 0$, it follows

$$\bar{b}(u,v,v) = 0. \tag{3.9}$$

Similarly,

$$L(w,\psi) \leq \|p_0\|_{L^2(\Sigma_0)} \|w\|_{L^2(\Sigma_0)} + \|q_0\|_{L^2(\Sigma_r)} \|\psi\|_{L^2(\Sigma_r)}$$

$$\leq C(\|p_0\|_{L^2(\Sigma_0)}, \|q_0\|_{L^2(\Sigma_r)}) (\|w\|_{L^2(\Sigma_0)} + \|\psi\|_{L^2(\Sigma_r)}). \tag{3.10}$$

To deal with the non-homogeneous boundary conditions for the Navier–Stokes equations, we let $u_0 \in (H^{1/2}(\Sigma_i))^3$, $p_0 \in L^2(\Sigma_o)$, and assume that there exits a function $\tilde{u} \in (H^1(\Omega_f))^3$ such that

$$\nabla \cdot \tilde{u} = 0 \quad \text{in } \Omega_{f}, \tag{3.11}$$

$$\tilde{u} = 0$$
 on $\Sigma_{\rm w}$, $\tilde{u} = u_0$ on $\Sigma_{\rm i}$, and $\tilde{u} \times n_{\rm o} = 0$ on $\Sigma_{\rm o}$. (3.12)

Moreover, by trace theorem we get

$$\|\tilde{u}\|_{H^{1}(\Omega_{f})} \leqslant c_{0} \|u_{0}\|_{H^{1/2}(\Sigma_{f})} \tag{3.13}$$

for some constant $c_0 > 0$. The existence of $\tilde{u} \in (H^1(\Omega_f))^3$ satisfying (3.11) and (3.12) will not be addressed here. The detailed discussion for this problem with smooth domains and Dirichlet boundary conditions can be found in [63, chapter 2], and with Lipschitz domains and mixed boundary conditions can be found in (e.g. [14, 20, 43, 48]). We shall simply study (2.1)–(2.12) assuming the existence of \tilde{u} satisfying (3.11) and (3.12).

The following lemma can be established by slightly modifying the proof of [20, lemma 2.3, chapter IV] for Lipschitz domains.

Lemma 3.2. There exists $\tilde{u} = \tilde{u}(\gamma_0)$ satisfying (3.11) and (3.12) such that

$$\bar{b}(\bar{u}, \tilde{u}, \bar{u}) \leqslant \gamma_0 \|\bar{u}\|_{H^1(\Omega_c)}^2,\tag{3.14}$$

for every $\gamma_0 > 0$.

Note that the velocity u we are seeking for satisfies $u - \tilde{u} \in V_0^1(\Omega_f)$. Making a change of variable by letting

$$\bar{u} = u - \tilde{u},\tag{3.15}$$

the weak form (3.4) becomes

$$\bar{a}((\bar{u}+\tilde{u},\phi);(w,\psi))+\bar{b}(\bar{u}+\tilde{u},\bar{u}+\tilde{u},w)=L(w,\psi),$$

where

$$\bar{a}((\bar{u}+\tilde{u},\phi);(w,\psi)) = \bar{a}((\bar{u},\phi);(w,\psi)) + \bar{a}((\tilde{u},0);(w,\psi))$$

and

$$\bar{b}(\bar{u} + \tilde{u}, \bar{u} + \tilde{u}, w) = \bar{b}(\bar{u}, \bar{u}, w) + \bar{b}(\bar{u}, \tilde{u}, w) + \bar{b}(\tilde{u}, \bar{u}, w) + \bar{b}(\tilde{u}, \tilde{u}, w).$$

In other words, we seek for $(\bar{u}, \phi) \in V$ satisfying the following weak formulation

$$\bar{a}((\bar{u},\phi);(w,\psi)) + \bar{b}(\bar{u},\tilde{u},w) + \bar{b}(\tilde{u},\bar{u},w) + \bar{b}(\bar{u},\bar{u},w)$$

$$= L(w,\psi) - \bar{a}((\tilde{u},0);(w,\psi)) - \bar{b}(\tilde{u},\tilde{u},w), \quad \forall (w,\psi) \in V.$$
(3.16)

3.1. Well-posedness of the steady-state Navier-Stokes-Darcy problem

Definition 3.3. Let $u_0 \in H^{1/2}(\Sigma_i)$, $p_0 \in L^2(\Sigma_0)$, $q_0 \in L^2(\Sigma_r)$ and $(\kappa, \beta) \in \mathbb{K} \times \mathbb{R}^+$. $(u, \phi) \in V^1_{u_0}(\Omega_s) \times H^1(\Omega_s)$ is said to be a weak solution of equations (2.1)–(2.12), if $\bar{u} = u - \tilde{u} \in V^1_0(\Omega)$ and (\bar{u}, ϕ) satisfies (3.16) for any $(w, \psi) \in V$.

The following theorem establish the well-posedness of the weak form (3.16).

Theorem 3.1. For given ρ , μ , β , $\kappa_l > 0$, let $u_0 \in H^{1/2}(\Sigma_i)$, $p_0 \in L^2(\Sigma_0)$, $q_0 \in L^2(\Sigma_r)$, and $\kappa \in \mathbb{K}$. Then there exists at least one solution $(\bar{u}, \phi) \in V$ to the weak formulation (3.16). Moreover,

$$\|\bar{u}\|_{H^{1}(\Omega_{f})} + \|\phi\|_{H^{1}(\Omega_{s})} \leq C(\|u_{0}\|_{H^{1/2}(\Sigma_{i})}, \|p_{0}\|_{L^{2}(\Sigma_{0})}, \|q_{0}\|_{L^{2}(\Sigma_{r})}), \tag{3.17}$$

and hence

$$||u||_{H^{1}(\Omega_{f})} + ||\phi||_{H^{1}(\Omega_{s})} \leq C_{u}(||u_{0}||_{H^{1/2}(\Sigma_{t})}, ||p_{0}||_{L^{2}(\Sigma_{0})}, ||q_{0}||_{L^{2}(\Sigma_{f})}),$$
(3.18)

for some constants C and C_u depending on the model input data u_0, p_0, q_0 , and the parameters ρ , μ , β , and κ_l .

The uniqueness of the solution can be obtained using the similar procedures as in (e.g. [13, 63]) by imposing large Reynolds number μ and permeability κ or small data of the model, i.e., u_0, p_0, q_0, β .

4. Existence of an optimal solution

In this section, we address the existence of an optimal solution to problem (P). Note that the uniqueness of the solution to the 3D steady state Navier–Stokes–Darcy model can be obtained for small data (similar to conditions used in [63, theorem 1.6, chapter II, p 120]). However, uniqueness of the state equations is not required for the existence of a solution to an optimization problem.

Define $\|\kappa\|_{\mathbb{K}}^2 = \|\nabla\kappa\|_{L^2(\Omega_\epsilon)}^2 + \|\kappa\|_{L^2(\Omega_\epsilon)}^2$. Then the cost functional J can be rewritten as

$$J(\kappa) = \frac{1}{2} \|\mathcal{C}u - y_{\text{ref}}\|_{\mathcal{Y}}^2 + \frac{\alpha}{2} (\|\kappa\|_{L^2(\Omega_s)}^2 + \|\nabla\kappa\|_{L^2(\Omega_s)}^2), \quad \kappa_l \leqslant \kappa \leqslant \kappa_u.$$
 (4.1)

Theorem 4.1. Let $u_0 \in H^{1/2}(\Sigma_i)$, $p_0 \in L^2(\Sigma_o)$, $q_0 \in L^2(\Sigma_r)$. There exists an optimal solution $\kappa \in \mathbb{K}$ to problem (P).

Proof. Since $J(\cdot)$ is bounded from below, we can choose a minimizing sequence $\{\kappa_n\} \subset \mathbb{K}$ such that

$$\lim_{n \to \infty} J(\kappa_n) = \inf_{\kappa \in \mathbb{K}} J(\kappa). \tag{4.2}$$

By the definition of $J(\cdot)$, the sequence $\{k_n\}$ is uniformly bounded in \mathbb{K} , and hence there exists a subsequence, still denoted by $\{k_n\}$, such that

$$k_n \to k^*$$
 weakly in $H^1(\Omega_s)$
 $k_n \to k^*$ strongly in $H^{1/2}(\Omega_s)$ and $L^2(\Omega_s)$. (4.3)

For $u_0 \in H^{1/2}(\Sigma_i)$, $p_0 \in L^2(\Sigma_0)$, $q_0 \in L^2(\Sigma_r)$, let $\{(u_n, \phi_n)\}$ be a corresponding weak solution of the state equations (2.1)–(2.12) based on definition 3.3. Let $\bar{u}_n = u_n - \tilde{u}$. According to (3.17), $\{(\bar{u}_n, \phi_n)\}$ is bounded in V, thus there exists a subsequence, still denoted by $\{(\bar{u}_n, \phi_n)\}$ such that

$$(\bar{u}_n, \phi_n) \to (\bar{u}^*, \phi^*)$$
 weakly in V , (4.4)

$$(\bar{u}_n, \phi_n) \to (\bar{u}^*, \phi^*)$$
 strongly in $L^2(\Omega_f) \times L^2(\Omega_s)$. (4.5)

Let $u^* = \bar{u}^* + \tilde{u}$. Next we verify that (u^*, ϕ^*) is the solution associated with κ^* based on definition 3.3. Note that (\bar{u}_n, ϕ_n) satisfies

$$\bar{a}((\bar{u}_n, \phi_n); (w, \psi)) + b(\bar{u}_n, \bar{u}_n, w) = L(p_0, q_0) + \bar{a}(\tilde{u}, 0; (w, \psi)) - b(\bar{u}_n, \tilde{u}, w) - b(\tilde{u}, \bar{u}_n, w) - b(\tilde{u}, \tilde{u}, w),$$
(4.6)

for any $(w,\psi) \in (C^{\infty}(\overline{\Omega}_{\mathrm{f}}) \cap V_0^0(\Omega_{\mathrm{f}})) \times C^{\infty}(\overline{\Omega}_{\mathrm{f}})$. Due to the strong converge of $(\bar{u}_n,\phi_n) \in L^2(\Omega_{\mathrm{f}}) \times L^2(\Omega_{\mathrm{s}})$, it is straightforward to pass to the limit in the linear terms of $\bar{a}((\bar{u}_n,\phi_n);(w,\psi))$, $b(\bar{u}_n,\tilde{u},w)$ and $b(\tilde{u},\bar{u}_n,w)$. In light of (3.5) and (3.6), it remains to show that passing limit in the following nonlinear terms are possible

$$I_1(\kappa_n, \bar{u}_n) = \int_{\Sigma_c} \frac{\beta \mu}{\sqrt{\kappa_n}} (P_{\tau} \bar{u}_n) \cdot (P_{\tau} w) dx,$$

$$I_2(\kappa_n, \phi_n) = \int_{\Omega} \frac{\kappa_n}{\mu} \nabla \phi_n \cdot \nabla \psi \, dx,$$

and

$$I_3(\bar{u}_n) = \int_{\Omega_f} \rho((\nabla \times \bar{u}_n) \times \bar{u}_n) \cdot w \, \mathrm{d}x.$$

First, note that

$$|I_{1}(\kappa_{n},\phi_{n}) - I_{1}(\kappa^{*},\phi^{*})| = \left| \int_{\Sigma_{c}} \left(\frac{\beta\mu}{\sqrt{\kappa_{n}}} (P_{\tau}\bar{u}_{n}) - \frac{\beta\mu}{\sqrt{\kappa^{*}}} (P_{\tau}\bar{u}^{*}) \right) \cdot (P_{\tau}w) dx \right|$$

$$= \left| \int_{\Sigma_{c}} \left(\frac{\beta\mu}{\sqrt{\kappa_{n}}} (P_{\tau}\bar{u}_{n}) - \frac{\beta\mu}{\sqrt{\kappa_{n}}} (P_{\tau}\bar{u}^{*}) \right) \cdot (P_{\tau}w) dx \right|$$

$$+ \frac{\beta\mu}{\sqrt{\kappa_{n}}} (P_{\tau}\bar{u}^{*}) - \frac{\beta\mu}{\sqrt{\kappa^{*}}} (P_{\tau}\bar{u}^{*}) \right) \cdot (P_{\tau}w) dx \right|$$

$$= \left| \int_{\Sigma_{c}} \left(\frac{\beta\mu}{\sqrt{\kappa_{n}}} (P_{\tau}\bar{u}_{n} - P_{\tau}\bar{u}^{*}) + \beta\mu \left(\frac{1}{\sqrt{\kappa_{n}}} \right) \right) \cdot (P_{\tau}w) dx \right|$$

$$\leq \frac{\beta\mu}{\sqrt{\kappa_{l}}} \langle P_{\tau}\bar{u}_{n} - P_{\tau}\bar{u}^{*}, P_{\tau}w \rangle_{(H_{00}^{1/2}(\Sigma_{c}))', H_{00}^{1/2}(\Sigma_{c})}$$

$$+ \beta\mu \left| \int_{\Sigma_{c}} \left(\frac{1}{\sqrt{\kappa_{n}}} - \frac{1}{\sqrt{\kappa^{*}}} \right) (P_{\tau}\bar{u}^{*}) \cdot (P_{\tau}w) dx \right|$$

$$\leq \frac{\beta\mu}{\sqrt{\kappa_{l}}} \|\bar{u}_{n} - \bar{u}^{*}\|_{L^{2}(\Omega_{f})} \|w\|_{H^{1}(\Omega_{f})}$$

$$+ \beta\mu \left| \int_{\Sigma_{c}} \left(\frac{1}{\sqrt{\kappa_{n}}} - \frac{1}{\sqrt{\kappa^{*}}} \right) (P_{\tau}\bar{u}^{*}) \cdot (P_{\tau}w) dx \right|, \tag{4.7}$$

where the first term on the right-hand side of (4.7) converges to zero due to (4.5). Here $H_{00}^{1/2}(\Sigma_c)$ is a non-closed subspace of $H^{1/2}(\Gamma_c)$ and has a continuous zero extension to $H^{1/2}(\Sigma_f)$ [41, p 66]. It can be equivalently defined as the restriction of $H^1(\Omega_f)$ to Σ_c , i.e., $H_{00}^{1/2}(\Sigma_c) = H^1(\Omega_f)|_{\Gamma_c}$. Moreover, since

$$\frac{1}{\sqrt{\kappa_n}} - \frac{1}{\sqrt{\kappa^*}} = \frac{\sqrt{\kappa^*} - \sqrt{\kappa_n}}{\sqrt{\kappa_n \kappa^*}} = \frac{(\kappa^* - \kappa_n)}{\sqrt{\kappa_n \kappa^*}(\sqrt{\kappa_n} + \sqrt{\kappa^*})},$$

by (4.3) we get

$$\begin{split} & \left| \int_{\Sigma_{c}} \frac{(\kappa^{*} - \kappa_{n})}{\sqrt{\kappa_{n} \kappa^{*}} (\sqrt{\kappa_{n}} + \sqrt{\kappa^{*}})} (P_{\tau} \bar{u}^{*}) \cdot (P_{\tau} w) \mathrm{d}x \right| \\ & \leqslant \left\| \frac{(\kappa^{*} - \kappa_{n})}{\sqrt{\kappa_{n} \kappa^{*}} (\sqrt{\kappa_{n}} + \sqrt{\kappa^{*}})} \right\|_{L^{2}(\partial \Omega_{s})} \|P_{\tau} \bar{u}^{*}\|_{L^{4}(\partial \Omega_{f})} \|P_{\tau} w\|_{L^{4}(\partial \Omega_{f})} \\ & \leqslant C \frac{\|\kappa^{*} - \kappa_{n}\|_{H^{1/2}(\Omega_{s})}}{2\kappa_{l}^{3/2}} \|\bar{u}^{*}\|_{H^{1/2}(\partial \Omega_{f})} \|w\|_{H^{1/2}(\partial \Omega_{f})} \\ & \leqslant C \frac{\|\kappa^{*} - \kappa_{n}\|_{H^{1/2}(\Omega_{s})}}{2\kappa_{l}^{3/2}} \|\bar{u}^{*}\|_{H^{1}(\Omega_{f})} \|w\|_{H^{1}(\Omega_{f})} \to 0, \end{split}$$

which follows

$$I_1(\kappa_n, \phi_n) \to I_1(\kappa^*, \phi^*).$$
 (4.8)

Next, given (3.18), (4.3) and (4.4), and $\nabla \psi \in L^{\infty}(\Omega_s)$, we have

$$\begin{aligned} &|I_{2}(\kappa_{n},\phi_{n}) - I_{2}(\kappa^{*},\phi^{*})| \\ &= \left| \int_{\Omega_{s}} \left(\frac{\kappa_{n}}{\mu} \nabla \phi_{n} - \frac{\kappa^{*}}{\mu} \nabla \phi^{*} \right) \cdot \nabla \psi \, \mathrm{d}x \right| \\ &= \frac{1}{\mu} \left| \int_{\Omega_{s}} \left((\kappa_{n} - \kappa^{*}) \nabla \phi_{n} + \kappa^{*} (\nabla \phi_{n} - \nabla \phi^{*}) \right) \cdot \nabla \psi \, \mathrm{d}x \right| \\ &\leq \frac{1}{\mu} \|\kappa_{n} - \kappa^{*}\|_{L^{2}(\Omega_{s})} \|\nabla \phi_{n}\|_{L^{2}(\Omega_{s})} \|\nabla \psi\|_{L^{\infty}(\Omega_{s})} \\ &+ \frac{1}{\mu} \left| \int_{\Omega_{s}} (\kappa^{*} (\nabla \phi_{n} - \nabla \phi^{*})) \cdot \nabla \psi \, \mathrm{d}x \right| \to 0, \end{aligned}$$

and hence

$$I_2(\kappa_n, \phi_n) \to I_2(\kappa^*, \phi^*).$$
 (4.9)

Lastly, recall that

$$\begin{split} I_{3}(\bar{u}_{n}) &= \int_{\Omega_{\mathrm{f}}} (\nabla \times \bar{u}_{n}) \times \bar{u}_{n} \cdot w \, \mathrm{d}x \\ &= \int_{\partial\Omega_{\mathrm{f}}} (\bar{u}_{ni}n_{i}) \bar{u}_{nj}w_{j} \, \mathrm{d}x - \int_{\Omega_{\mathrm{f}}} \bar{u}_{ni}\bar{u}_{ni}\partial_{i}w_{j} \, \mathrm{d}x - \frac{1}{2} \int_{\partial\Omega_{\mathrm{f}}} w_{i}n_{i}\bar{u}_{ni}\bar{u}_{ni} \, \mathrm{d}x, \end{split}$$

then it follows from (4.5) that

$$I_3(\bar{u}_n) \to I_3(\bar{u}^*).$$
 (4.10)

With the help of (4.7)–(4.10), we can pass to the limit in (4.6). Moreover, since $(C^{\infty}(\overline{\Omega}_{\mathrm{f}}) \cap V_0^0(\Omega_{\mathrm{f}})) \times C^{\infty}(\overline{\Omega}_{\mathrm{f}})$ is dense in V, we have

$$\bar{a}((\bar{u}^*, \phi^*); (w, \psi)) + b(\bar{u}^*, \bar{u}^*, w) = L(p_0, q_0) + \bar{a}(\tilde{u}, 0; (w, \psi))$$
$$-b(\bar{u}^*, \tilde{u}, w) - b(\tilde{u}, \bar{u}^*, w) - b(\tilde{u}, \tilde{u}, w)$$

hold for any $(w, \psi) \in V$. Therefore, (u^*, ϕ^*) is indeed the weak solution corresponding to κ^* . Finally, since the output measurement operator \mathcal{C} is bounded and the norm is weakly lower semicontinuous, we have

$$\|\mathcal{C}u^* - \vec{y}_{\text{ref}}\|_{\mathcal{Y}}^2 \leqslant \underline{\lim}_{n \to \infty} \|\mathcal{C}u_n - \vec{y}_{\text{ref}}\|_{\mathcal{Y}}^2$$

and

$$\|\kappa^*\|_{\mathbb{K}}^2 \leqslant \underline{\lim}_{n\to\infty} \|\kappa_n\|_{\mathbb{K}}^2.$$

Therefore,

$$J(\kappa^*) \leqslant \lim_{n \to \infty} \inf J(\kappa_n),$$

which indicates that κ^* is the optimal solution to problem (P). This completes the proof. \Box

5. Adjoint approach and optimality conditions

To establish the first-order optimality conditions for solving the optimal solution to problem (P), we utilize the variational inequality together with the adjoint method (e.g. [25, chapter 1, section 1.6.2], [40, p 10]). The variational inequality states that if κ^* is an optimal solution, then

$$J'(k^*) \cdot (\kappa - \kappa^*) \geqslant 0, \quad \forall \ \kappa \in \mathbb{K}.$$
 (5.1)

To interpret (5.1) explicitly, it is key to derive the adjoint system associated with problem (P).

5.1. First variation of the governing system

As a first step to derive the adjoint system, we examine the Gâteaux differentiability of the state $(u(\kappa), \phi(\kappa))$ with respect to $\kappa \in \mathbb{K}$ and establish the first variation of the state equations.

Lemma 5.1. For given $(u, \phi) \in V_{u_0}^1(\Omega_s) \times H^1(\Omega_s)$ and $h \in H^1(\Omega_s) \cap L^{\infty}(\Omega_s)$, there exists a unique solution $(v, z) \in V_0^1(\Omega_f) \times H^1(\Omega_s)$ to the following equations

$$\rho(v \cdot \nabla u + u \cdot \nabla v) = -\nabla \tilde{p} + \nabla \cdot (\mu(\nabla v + (\nabla v)^{\mathrm{T}})), \tag{5.2}$$

$$\nabla \cdot v = 0, \tag{5.3}$$

where $\tilde{p} \in L^2(\Omega)$, and

$$-\nabla \cdot \left(\frac{1}{\mu} h \nabla \phi\right) - \nabla \cdot \left(\frac{\kappa}{\mu} \nabla z\right) = 0, \tag{5.4}$$

with boundary conditions

$$v = 0 \quad on \ \Sigma_{\mathbf{w}}, \tag{5.5}$$

$$v = 0 \quad on \ \Sigma_{i}, \tag{5.6}$$

$$v \times n_{\rm o} = 0 \quad on \ \Sigma_{\rm o}, \tag{5.7}$$

$$\rho v^{\mathrm{T}} u + \tilde{p} - n_{\mathrm{sf}} \cdot \mathbf{T}(v) n_{\mathrm{sf}} = 0, \quad on \ \Sigma_{\mathrm{o}}.$$
 (5.8)

Moreover,

$$v \cdot n_{\rm sf} = \tilde{q} \cdot n_{\rm sf} \quad on \ \Sigma_{\rm c},$$
 (5.9)

$$\tilde{q} \cdot n_{\rm r} = 0 \quad on \ \Sigma_{\rm r},$$
 (5.10)

where

$$\tilde{q} = -\frac{1}{\mu}h\nabla\phi - \frac{\kappa}{\mu}\nabla z,\tag{5.11}$$

and

$$\rho v^{\mathrm{T}} u + \tilde{p} - n_{\mathrm{sf}} \cdot \mathbf{T}(v) n_{\mathrm{sf}} = z, \quad on \ \Sigma_{\mathrm{c}}. \tag{5.12}$$

The Beavers-Joseph-Saffman slip condition leads to

$$\tau_{\rm sf} \cdot \mathbf{T}(v) n_{\rm sf} = -\frac{\beta \mu}{2\kappa^{3/2}} h(u \cdot \tau_{\rm sf}) + \frac{\beta \mu}{\sqrt{\kappa}} (v \cdot \tau_{\rm sf}) \quad on \ \Sigma_{\rm c}. \tag{5.13}$$

The flow flux on the surface Γ_r becomes

$$\tilde{q} \cdot n_{\rm r} = 0 \quad on \ \Sigma_{\rm r}.$$
 (5.14)

Proof. It is easy to verify that the weak formulation of the equations (5.2)–(5.10) reads

$$\bar{a}_{var}((v,z);(w,\psi)) + \bar{b}(v,u,w) + \bar{b}(u,v,w) = 0,$$
 (5.15)

where $\bar{a}_{var}(\cdot;\cdot): V \times V \to \mathbb{R}$ is given by

$$\bar{a}_{var}((v,z);(w,\psi)) = \frac{1}{2\mu} \int_{\Omega_{\rm f}} \mathbf{T}(v) \cdot \mathbf{T}(w) \mathrm{d}x + \int_{\Sigma_{\rm c}} z(w \cdot n_{\rm fs}) \mathrm{d}x
- \int_{\Sigma_{\rm c}} \left(\frac{\beta\mu}{2\kappa^{3/2}}h\right) (P_{\tau}u) \cdot (P_{\tau}w) \mathrm{d}x + \int_{\Sigma_{\rm c}} \frac{\beta\mu}{\sqrt{\kappa}} (P_{\tau}v) \cdot (P_{\tau}w) \mathrm{d}x
+ \int_{\Sigma_{\rm c}} (v \cdot n_{\rm sf}) \psi \, \mathrm{d}x + \int_{\Omega_{\rm s}} \frac{1}{\mu} h(\nabla \phi \cdot \nabla \psi) \mathrm{d}x + \int_{\Omega_{\rm s}} \frac{\kappa}{\mu} \nabla z \cdot \nabla \psi \, \mathrm{d}x.$$
(5.16)

Based on (3.5) and (5.16), we can rewrite (5.15) as

$$\bar{a}((v,z);(w,\psi)) + \bar{b}(v,u,w) + \bar{b}(u,v,w) = \int_{\Sigma_{c}} \left(\frac{\beta\mu}{2\kappa^{3/2}}h\right) (P_{\tau}u) \cdot (P_{\tau}w) dx$$
$$-\int_{\Omega_{c}} \frac{1}{\mu} h(\nabla\phi \cdot \nabla\psi) dx. \tag{5.17}$$

Now let $(w, \psi) = (v, z)$. Then (5.17) becomes

$$\bar{a}((v,z);(v,z)) + \bar{b}(v,u,v) = \int_{\Sigma_{c}} \left(\frac{\beta\mu}{2\kappa^{3/2}}h\right) (P_{\tau}u) \cdot (P_{\tau}v) dx$$
$$-\int_{\Omega_{\tau}} \frac{1}{\mu} h(\nabla\phi \cdot \nabla z) dx. \tag{5.18}$$

Next, we show that the left-hand side of (5.18) is coercive. By (A.2) we have

$$\bar{a}((v,z);(v,z)) \geqslant \alpha_0(\|v\|_{H^1(\Omega_t)}^2 + \|z\|_{H^1(\Omega_t)}^2). \tag{5.19}$$

Moreover, using (3.8) together with Ladyzhenskaya and Young's inequalities, we get

$$\begin{split} \bar{b}(v, u, v) &\leqslant \rho \|\nabla v\|_{L^{2}(\Omega_{f})} \|u\|_{L^{4}(\Omega_{f})} \|v\|_{L^{4}(\Omega_{f})} \\ &\leqslant C \rho \|v\|_{H^{1}(\Omega_{f})} \|u\|_{H^{1}(\Omega_{f})} \|v\|_{L^{2}(\Omega_{f})}^{1/4} \|v\|_{H^{1}(\Omega_{f})}^{3/4} \\ &= C \rho \|u\|_{H^{1}(\Omega_{f})} D^{-1} (\|v\|_{L^{2}(\Omega_{f})}^{1/4} D \|v\|_{H^{1}(\Omega_{f})}^{7/4}) \\ &\leqslant C \rho \|u\|_{H^{1}(\Omega_{f})} D^{-1} \left(\frac{1}{8} \|v\|_{L^{2}(\Omega_{f})}^{2} + \frac{7}{8} (D^{8/7} \|v\|_{H^{1}(\Omega_{f})}^{2})\right) \\ &\leqslant C \rho \|u\|_{H^{1}(\Omega_{f})} D^{-1} \frac{1}{8} \|v\|_{L^{2}(\Omega_{f})}^{2} + \frac{7}{8} C \rho \|u\|_{H^{1}(\Omega_{f})} D^{1/7} \|v\|_{H^{1}(\Omega_{f})}^{2} \\ &\leqslant C (\rho, \alpha_{0}, \|u\|_{H^{1}(\Omega_{f})}) \|v\|_{L^{2}(\Omega_{f})}^{2} + \frac{\alpha_{0}}{4} \|v\|_{H^{1}(\Omega_{f})}^{2}, \end{split}$$
 (5.20)

where $D=(\frac{2\alpha_0}{7C\rho\|u\|_{H^1(\Omega_t)}})^7$. Thus, the coercivity of $\bar{a}((\cdot,\cdot);(\cdot,\cdot))+\bar{b}(\cdot,u,\cdot)$ follows, that is,

$$\begin{split} \bar{a}((v,z);(v,z)) + \bar{b}(v,u,v) + C(\rho,\alpha_0,\|u\|_{H^1(\Omega_{\mathrm{f}})})\|v\|_{L^2(\Omega_{\mathrm{f}})}^2 \\ &\geqslant \alpha_0(\|v\|_{H^1(\Omega_{\mathrm{f}})}^2 + \|z\|_{H^1(\Omega_{\mathrm{f}})}^2) \\ &- \left(C(\rho,\alpha_0,\|u\|_{H^1(\Omega_{\mathrm{f}})})\|v\|_{L^2(\Omega_{\mathrm{f}})}^2 + \frac{\alpha_0}{4}\|v\|_{H^1(\Omega_{\mathrm{f}})}^2\right) \end{split}$$

$$+ C(\rho, \alpha_0, ||u||_{H^1(\Omega_f)}) ||v||_{L^2(\Omega_f)}^2$$

$$\geq \frac{3}{4} \alpha_0 (||v||_{H^1(\Omega_f)}^2 + ||z||_{H^1(\Omega_f)}^2).$$
 (5.21)

Furthermore, the terms on the right-hand side of (5.18) satisfy

$$\left| \int_{\Sigma_{c}} \left(\frac{\beta \mu}{2\kappa^{3/2}} h \right) (P_{\tau}u) \cdot (P_{\tau}v) dx \right| \leq \frac{\beta \mu}{2\kappa_{l}^{3/2}} \|h\|_{L^{\infty}(\Omega_{s})} \|P_{\tau}u\|_{L^{2}(\Sigma_{c})} \|P_{\tau}v\|_{L^{2}(\Sigma_{c})}$$

$$\leq C_{\Sigma_{c}} \frac{\beta \mu}{\kappa_{l}^{3/2}} \|h\|_{L^{\infty}(\Omega_{s})} \|u\|_{H^{1}(\Omega_{f})} \|v\|_{H^{1}(\Omega_{f})}$$
(5.22)

for some constant $C_{\Sigma_c} > 0$ depending only on Ω_f , and

$$\left| \int_{\Omega_s} \frac{1}{\mu} h(\nabla \phi \cdot \nabla z) \mathrm{d}x \right| \leqslant \frac{1}{\mu} \|h\|_{L^{\infty}(\Omega_s)} \|\phi\|_{H^1(\Omega_s)} \|z\|_{H^1(\Omega_f)}. \tag{5.23}$$

Therefore, by (5.18), (5.22) and (5.23) we have

$$\bar{a}((v,z);(v,z)) + \bar{b}(v,u,v)
\leq C(\mu,\beta,\kappa_l, \|u\|_{H^1(\Omega_t)}, \|\phi\|_{H^1(\Omega_t)}) \|h\|_{L^{\infty}(\Omega_t)} (\|v\|_{H^1(\Omega_t)} + \|z\|_{H^1(\Omega_t)}).$$

The existence of a unique solution follows immediately from Lax–Milgram theorem. This completes the proof. \Box

Lemma 5.2. For given $\rho, \mu, \beta, k_l, k_u > 0$, let $u_0 \in H^{1/2}(\Sigma_i), p_0 \in L^2(\Sigma_o)$ and $q_0 \in L^2(\Sigma_r)$ be sufficiently small such that $\|u\|_{H^1(\Omega_f)}$ is sufficiently small. Then the mapping $\kappa \mapsto (u, \phi)$, from \mathbb{K} to V has a Gâteaux derivative $(u'(\kappa), \phi'(\kappa))$ in every feasible direction $h \in H^1(\Omega_s) \cap L^{\infty}(\Omega_s)$. Moreover, if letting $(v(\kappa), z(\kappa)) = (u'(\kappa) \cdot h, \phi'(\kappa) \cdot h)$, then there exists $\tilde{q}(k) = q'(\kappa) \cdot h \in L^2(\Omega_f)$ such that (v(k), z(k)) satisfies the equations (5.2)–(5.10).

Proof. To start with, we let $\Phi(k) = (u(\kappa), \phi(\kappa)), \ \Psi(\kappa) = (v(\kappa), z(\kappa)) = (u'(\kappa) \cdot h, \phi'(\kappa) \cdot h)$, and show that $\Phi(k)$ is locally Gâteaux differentiable at $\kappa \in \mathbb{K}$ in the feasible direction $h \in H^1(\Omega_s) \cap L^{\infty}(\Omega_s)$, that is,

$$\min_{\lambda \to 0} \frac{\left| \Phi(\kappa + \lambda h) - \Phi(\kappa) - \lambda \Psi(\kappa) \right|}{|\lambda|} = 0, \tag{5.24}$$

for $\forall 0 \neq \lambda \in \mathbb{R}$ such that $\kappa + \lambda h \in \mathbb{K}$. Using (3.4)–(3.7) and (5.17), it is straightforward to verify that $\Phi(\kappa + \lambda h) - \Phi(\kappa) - \lambda \Psi(\kappa)$ satisfies the following weak formulation

$$0 = \bar{a}((u(\kappa + \lambda h), \phi(\kappa + \lambda h)); (w, \psi)) + \bar{b}(u(\kappa + \lambda h), u(\kappa + \lambda h), w)$$

$$- [\bar{a}((u(\kappa), \phi(\kappa)); (w, \psi)) + \bar{b}(u(\kappa), u(\kappa), w)]$$

$$- \lambda \left[\bar{a}((v(\kappa), z(\kappa)); (w, \psi)) + \bar{b}(v(\kappa), u(\kappa), w) + \bar{b}(u(\kappa), v(\kappa), w) \right]$$

$$- \left(\int_{\Sigma_{c}} \left(\frac{\beta \mu}{2\kappa^{3/2}} h \right) (P_{\tau} u(\kappa)) \cdot (P_{\tau} w) dx - \int_{\Omega_{s}} \frac{1}{\mu} h(\nabla \phi(\kappa) \cdot \nabla \psi) dx \right) \right],$$
(5.25)

where

$$\bar{b}(u(\kappa + \lambda h), u(\kappa + \lambda h), w) - \bar{b}(u(\kappa), u(\kappa), w)
- \lambda(\bar{b}(v(\kappa), u(\kappa), w) + \bar{b}(u(\kappa), v(\kappa), w))
= \bar{b}(u(\kappa + \lambda h) - u(\kappa) - \lambda v(\kappa), u(k + \lambda h), w)
+ \bar{b}(u(\kappa), u(\kappa + \lambda h) - u(\kappa) - \lambda v(\kappa), w)
+ \lambda \bar{b}(v(\kappa), u(k + \lambda h) - u(\kappa), w)$$
(5.26)

and

$$\bar{a}((u(\kappa + \lambda h), \phi(\kappa + \lambda h)); (w, \psi)) - \bar{a}((u(\kappa), \phi(\kappa)); (w, \psi))
- \lambda \bar{a}((v(\kappa), z(\kappa)); (w, \psi))
= \bar{a}((u(\kappa + \lambda h) - u(\kappa) - \lambda v(\kappa), \phi(\kappa + \lambda h) - \phi(\kappa) - \lambda z(\kappa)); (w, \psi))
+ \left(\int_{\Sigma_{c}} \left(\frac{\beta \mu}{\sqrt{\kappa + \lambda h}} - \frac{\beta \mu}{\sqrt{\kappa}}\right) P_{\tau}(u(\kappa + \lambda h)) \cdot (P_{\tau}w) dx\right)
+ \left(\int_{\Omega_{c}} \frac{\lambda}{\mu} h(\nabla \phi(\kappa + \lambda h) \cdot \nabla \psi) dx\right).$$
(5.27)

Combining (5.25) with (5.26) and (5.27) follows

$$0 = \bar{a}((u(\kappa + \lambda h) - u(\kappa) - \lambda v(\kappa), \phi(\kappa + \lambda h) - \phi(\kappa) - \lambda z(\kappa)); (w, \psi))$$

$$+ \left(\int_{\Sigma_{c}} \left(\frac{\beta \mu}{\sqrt{\kappa + \lambda h}} - \frac{\beta \mu}{\sqrt{\kappa}}\right) P_{\tau}(u(\kappa + \lambda h)) \cdot (P_{\tau}w) dx\right)$$

$$+ \left(\int_{\Omega_{s}} \frac{\lambda}{\mu} h(\nabla \phi(\kappa + \lambda h) \cdot \nabla \psi) dx\right) + \bar{b}(u(\kappa + \lambda h) - u(\kappa)$$

$$- \lambda v(\kappa), u(k + \lambda h), w) + \bar{b}(u(\kappa), u(\kappa + \lambda h) - u(\kappa) - \lambda v(\kappa), w)$$

$$+ \lambda \bar{b}(v(\kappa), u(k + \lambda h) - u(\kappa), w) + \lambda \left(\int_{\Sigma_{c}} \left(\frac{\beta \mu}{2\kappa^{3/2}} h\right)\right)$$

$$\times (P_{\tau}u(\kappa)) \cdot (P_{\tau}w) dx - \int_{\Omega_{s}} \frac{1}{\mu} h(\nabla \phi(\kappa) \cdot \nabla \psi) dx\right)$$

$$= \bar{a}((u(\kappa + \lambda h) - u(\kappa) - \lambda v(\kappa), \phi(\kappa + \lambda h) - \phi(\kappa) - \lambda z(\kappa)); (w, \psi))$$

$$+ \left(\int_{\Sigma_{c}} \left(\frac{\beta \mu}{\sqrt{\kappa + \lambda h}} - \frac{\beta \mu}{\sqrt{\kappa}} + \lambda \frac{\beta \mu}{2\kappa^{3/2}} h\right) P_{\tau}(u(\kappa + \lambda h)) \cdot (P_{\tau}w) dx\right)$$

$$+ \left(\int_{\Omega_{s}} \frac{\lambda}{\mu} h(\nabla (\phi(\kappa + \lambda h) - \phi(k)) \cdot \nabla \psi) dx\right) + \bar{b}(u(\kappa + \lambda h) - u(\kappa) - \lambda v(\kappa),$$

$$\times u(k + \lambda h), w) + \bar{b}(u(\kappa), u(\kappa + \lambda h) - u(\kappa) - \lambda v(\kappa), w) + \lambda \bar{b}(v(\kappa), u(k + \lambda h) - u(\kappa), w) - \lambda \int_{\Sigma_{c}} \left(\frac{\beta \mu}{2\kappa^{3/2}} h\right) (P_{\tau}(u(k + \lambda h) - u(\kappa)) \cdot (P_{\tau}w) dx. \tag{5.28}$$

To simplify the expression, we let $R = u(\kappa + \lambda h) - u(\kappa) - \lambda v(\kappa)$, $H = \phi(\kappa + \lambda h) - \phi(\kappa) - \lambda z(\kappa)$ and set $(w, \psi) = (R, H)$. Then (5.28) becomes

$$0 = \bar{a}((R, H); (R, H))$$

$$+ \left(\int_{\Sigma_{c}} \left(\frac{\beta \mu}{\sqrt{\kappa + \lambda h}} - \frac{\beta \mu}{\sqrt{\kappa}} + \lambda \frac{\beta \mu}{2\kappa^{3/2}} h \right) P_{\tau}(u(\kappa + \lambda h)) \cdot (P_{\tau}R) dx \right)$$

$$+ \int_{\Omega_{s}} \frac{\lambda}{\mu} h \left(\nabla (\phi(\kappa + \lambda h) - \phi(k)) \cdot \nabla H dx \right)$$

$$+ \bar{b}(R, u(k + \lambda h), R) + \bar{b}(u(\kappa), R, R) + \lambda \bar{b}(v(\kappa), R + \lambda v(\kappa), R)$$

$$- \lambda \left(\int_{\Sigma_{c}} \left(\frac{\beta \mu}{2\kappa^{3/2}} h \right) \left(P_{\tau}(u(\kappa + \lambda h) - u(\kappa)) \cdot (P_{\tau}R) dx \right),$$
 (5.29)

where $\bar{b}(u(\kappa), R, R) = 0$ and $\lambda \bar{b}(v(\kappa), R + \lambda v(\kappa), R) = \lambda^2 \bar{b}(v(\kappa), v(\kappa), R)$.

In the next step, we show that $\delta u = u(\kappa + \lambda h) - u(\kappa)$ and $\delta \phi = \phi(\kappa + \lambda h) - \phi(k)$ are of order λ . First, based on (3.4) we have

$$0 = \bar{a}((u(\kappa + \lambda h), \phi(\kappa + \lambda h)); (w, \psi)) + \bar{b}(u(\kappa + \lambda h), u(\kappa + \lambda h), w)$$
$$- [\bar{a}((u(\kappa), \phi(\kappa)); (w, \psi)) + \bar{b}(u(\kappa), u(\kappa), w)], \tag{5.30}$$

where

$$\bar{a}((u(\kappa + \lambda h), \phi(\kappa + \lambda h)); (w, \psi)) - \bar{a}((u(\kappa), \phi(\kappa)); (w, \psi))$$

$$= \bar{a}((u(\kappa + \lambda h) - u(\kappa), \phi(\kappa + \lambda h) - \phi(\kappa)); (w, \psi))$$

$$+ \left(\int_{\Sigma_{c}} \left(\frac{\beta \mu}{\sqrt{\kappa + \lambda h}} - \frac{\beta \mu}{\sqrt{\kappa}}\right) P_{\tau}(u(\kappa + \lambda h)) \cdot (P_{\tau} w) dx\right)$$

$$+ \left(\int_{\Omega} \frac{\lambda}{\mu} h(\nabla \phi(\kappa + \lambda h) \cdot \nabla \psi) dx\right) \tag{5.31}$$

and

$$\bar{b}(u(\kappa + \lambda h), u(\kappa + \lambda h), w) - \bar{b}(u(\kappa), u(\kappa), w)$$

$$= \bar{b}(u(\kappa + \lambda h) - u(\kappa), u(k + \lambda h), w) + \bar{b}(u(\kappa), u(\kappa + \lambda h) - u(\kappa), w).$$
(5.32)

Substituting (5.32) and (5.31) into (5.30), given $\bar{b}(u(\kappa), \delta u, \delta u) = 0$, and setting $(w, \psi) = (\delta u, \delta \phi)$ lead to

$$0 = \bar{a}((\delta u, \delta \phi); (\delta u, \delta \phi)) + \bar{b}(\delta u, u(k + \lambda h), \delta u)$$

$$+ \left(\int_{\Sigma_{c}} \left(\frac{\beta \mu}{\sqrt{\kappa + \lambda h}} - \frac{\beta \mu}{\sqrt{\kappa}} \right) P_{\tau}(u(\kappa + \lambda h)) \cdot (P_{\tau} \delta u) dx \right)$$

$$+ \left(\int_{\Omega_{s}} \frac{\lambda}{\mu} h(\nabla \phi(\kappa + \lambda h) \cdot \nabla \psi) dx \right).$$

Applying (3.18), (5.22) and (A.2) that $\|u(\kappa + \lambda h)\|_{H^1(\Omega_f)} + \|\phi(u + \lambda h)\|_{H^1(\Omega_s)} \leq C_u$, we have

$$\begin{split} &\alpha_{0}(\|\delta u\|_{H^{1}(\Omega_{\mathrm{f}})}^{2} + \|\delta\phi\|_{H^{1}(\Omega_{\mathrm{s}})}^{2}) \\ &\leqslant \bar{a}((\delta u, \delta\phi); (\delta u, \delta\phi)) \\ &\leqslant |\bar{b}(\delta u, u(k + \lambda h), \delta u)| \\ &+ \left| \int_{\Sigma_{\mathrm{c}}} \left(\frac{\beta \mu}{\sqrt{\kappa + \lambda h}} - \frac{\beta \mu}{\sqrt{\kappa}} \right) P_{\tau}(u(\kappa + \lambda h)) \cdot (P_{\tau} \delta u) \mathrm{d}x \right| \\ &+ \left| \int_{\Omega_{\mathrm{s}}} \frac{\lambda}{\mu} h(\nabla \phi(\kappa + \lambda h) \cdot \nabla \delta \phi) \mathrm{d}x \right| \\ &\leqslant C_{\bar{b}} \rho \|u(k + \lambda h)\|_{H^{1}(\Omega)} \|\delta u\|_{H^{1}(\Omega)}^{2} \\ &+ C_{\Sigma_{\mathrm{c}}} \left\| \frac{\beta \mu}{\sqrt{\kappa + \lambda h}} - \frac{\beta \mu}{\sqrt{\kappa}} \right\|_{L^{\infty}(\Omega_{\mathrm{s}})} \|u(\kappa + \lambda h)\|_{H^{1}(\Omega_{\mathrm{f}})} \|\delta u\|_{H^{1}(\Omega_{\mathrm{f}})} \\ &+ |\lambda| \frac{\|h\|_{L^{\infty}(\Omega_{\mathrm{s}})}}{\mu} \|\phi(\kappa + \lambda h)\|_{\mathcal{H}^{1}(\Omega_{\mathrm{s}})} \|\delta\phi\|_{\mathcal{H}^{1}(\Omega_{\mathrm{s}})} \\ &\leqslant C_{\bar{b}} \rho C_{u} \|\delta u\|_{H^{1}(\Omega)}^{2} + C_{\Sigma_{\mathrm{c}}} |\lambda| \|h\|_{L^{\infty}(\Omega_{\mathrm{s}})} \frac{\beta \mu}{2\kappa_{l}^{3/2}} C_{u} \|\delta u\|_{H^{1}(\Omega_{\mathrm{f}})} \\ &+ |\lambda| \|h\|_{L^{\infty}(\Omega_{\mathrm{s}})} \frac{1}{\mu} C_{u} \|\delta\phi\|_{\mathcal{H}^{1}(\Omega_{\mathrm{s}})} \end{split}$$

which follows

$$(\alpha_{0} - C_{\bar{b}}\rho C_{u})(\|\delta u\|_{H^{1}(\Omega_{f})}^{2} + \|\delta\phi\|_{H^{1}(\Omega_{s})}^{2})$$

$$\leq C_{u} \left(C_{\Sigma_{c}} \frac{\beta\mu}{2\kappa_{l}^{3/2}} + \frac{1}{\mu} \right) |\lambda| \|h\|_{L^{\infty}(\Omega_{s})} (\|\delta u\|_{H^{1}(\Omega_{f})}^{2} + \|\delta\phi\|_{H^{1}(\Omega_{s})}^{2})^{1/2}. \quad (5.33)$$

According to (A.5), we know that $\|u(\kappa + \lambda h)\|_{H^1(\Omega_f)}$ and $\|\phi(\kappa + \lambda h)\|_{H^1(\Omega_s)}$ can be arbitrarily small by letting $\|u_0\|_{H^{1/2}(\Sigma_i)}$, $\|p_0\|_{L^2(\Sigma_0)}$, and $\|q_0\|_{L^2(\Sigma_r)}$ be small enough. In particular, if u_0 , p_0 and q_0 are chosen such that

$$C_u < \frac{\alpha_0}{C_{\bar{b}}\rho},\tag{5.34}$$

then $\alpha_0 - C_{\bar{h}}\rho C_u > 0$, and therefore,

$$(\|\delta u\|_{H^{1}(\Omega_{f})}^{2} + \|\delta \phi\|_{H^{1}(\Omega_{s})}^{2})^{1/2} \leqslant C_{h}|\lambda|\|h\|_{L^{\infty}(\Omega_{s})}, \tag{5.35}$$

for some constant $C_h > 0$. Now substituting (5.22), (5.33) and (A.2) into (5.29) yields

$$\alpha_{0}(\Vert R \Vert_{H^{1}(\Omega_{f})}^{2} + \Vert H \Vert_{H^{1}(\Omega_{s})}^{2})$$

$$\leqslant \bar{a}((R, H); (R, H))$$

$$\leqslant \left| \int_{\Sigma_{c}} \left(\frac{\beta \mu}{\sqrt{\kappa + \lambda h}} - \frac{\beta \mu}{\sqrt{\kappa}} + \lambda \frac{\beta \mu}{2\kappa^{3/2}} h \right) P_{\tau}(u(\kappa + \lambda h)) \cdot (P_{\tau}R) dx \right|$$

$$+ \left| \int_{\Omega_{s}} \frac{\lambda}{\mu} h(\nabla \delta \phi(k) \cdot \nabla H) dx \right|$$

$$+ \left| \bar{b}(R, u(k + \lambda h), R) \right| + \lambda^{2} \left| \bar{b}(v(\kappa), v(\kappa), R) \right|$$

$$+ \left| \lambda \right| \left| \int_{\Sigma_{c}} \left(\frac{\beta \mu}{2\kappa^{3/2}} h \right) (P_{\tau} \delta u) \cdot (P_{\tau}R) dx \right|$$

$$\leqslant C_{\Sigma_{c}} C_{u} \left\| \frac{\beta \mu}{\sqrt{\kappa + \lambda h}} - \frac{\beta \mu}{\sqrt{\kappa}} + \lambda \frac{\beta \mu}{2\kappa^{3/2}} h \right\|_{L^{\infty}(\Omega_{s})} \|R\|_{H^{1}(\Omega_{f})}$$

$$+ \frac{\lambda^{2}}{\mu} \|h\|_{L^{\infty}(\Omega_{s})}^{2} C_{h} \|H\|_{H^{1}(\Omega_{s})}$$

$$+ C_{\bar{b}} \rho C_{u} \|R\|_{H^{1}(\Omega)}^{2} + \lambda^{2} C_{\bar{b}} \rho \|v(\kappa)\|_{H^{1}(\Omega_{f})}^{2} \|R\|_{H^{1}(\Omega_{f})}$$

$$+ \lambda^{2} \|h\|_{L^{\infty}(\Omega_{s})}^{2} C_{\Sigma_{c}} C_{h} \left(\frac{\beta \mu}{2\kappa_{h}^{3/2}} \right) \|R\|_{H^{1}(\Omega_{f})}, \tag{5.36}$$

where $\left\|\frac{\beta\mu}{\sqrt{\kappa+\lambda h}}-\frac{\beta\mu}{\sqrt{\kappa}}+\lambda\frac{\beta\mu}{2\kappa^{3/2}}h\right\|_{L^{\infty}(\Omega_{s})}\leqslant \frac{3\beta\mu}{8k_{l}^{5/2}}\lambda^{2}\|h\|_{L^{\infty}(\Omega_{s})}^{2}$ based on Taylor's expansion. Thus from (5.36) we get

$$(\alpha_{0} - C_{\bar{b}}\rho C_{u})\|(R, H)\|^{2} \leqslant \lambda^{2} \left(C_{\Sigma_{c}} C_{u} \frac{3\beta\mu}{8k_{l}^{5/2}} \|h\|_{L^{\infty}(\Omega_{s})}^{2} + \frac{1}{\mu} C_{h} \|h\|_{L^{\infty}(\Omega_{s})}^{2} + C_{\bar{b}}\rho \|v(\kappa)\|_{H^{1}(\Omega_{f})}^{2} + C_{h} C_{\Sigma_{c}} \left(\frac{\beta\mu}{2\kappa_{l}^{3/2}} \right) \|h\|_{L^{\infty}(\Omega_{s})}^{2} \right) \|(R, H)\|, \quad (5.37)$$

where $\|(R, H)\| = (\|R\|_{H^1(\Omega_f)}^2 + \|H\|_{H^1(\Omega_s)}^2)^{1/2}$. Note that by lemma 5.1 we have $v \in V_0^1(\Omega_f)$. Therefore, (5.37) indicates that

$$||(R,H)|| \leqslant C\lambda^2,\tag{5.38}$$

for some constant C > 0, and hence (5.24) holds. This completes the proof.

5.2. Adjoint system

With the understanding of the first variation of $(u(\kappa), \phi(\kappa))$ with respect to $\kappa \in \mathbb{K}$, we proceed to derive the adjoint system associated with problem (P).

Theorem 5.1. Let (w, ψ) be the adjoint state. Then it satisfies the following equations

$$\rho((\nabla u)^{\mathrm{T}}w - u \cdot \nabla w) + \nabla Q - \nabla \cdot (\mu(\nabla w + (\nabla w)^{\mathrm{T}})) = \mathcal{C}^{*}(\mathcal{C}u - y_{\mathrm{ref}}), \quad (5.39)$$

$$\nabla \cdot w = 0, \tag{5.40}$$

$$-\nabla \cdot \left(\frac{\kappa}{\mu} \nabla \psi\right) = 0, \tag{5.41}$$

with boundary conditions

$$w = 0 \quad on \ \Sigma_{i} \cup \Sigma_{w}, \tag{5.42}$$

$$Q - n_0 \cdot \mathbf{T}(w) n_0 = 0 \quad on \ \Sigma_0, \tag{5.43}$$

$$w \times n_0 = 0 \quad on \ \Sigma_0, \tag{5.44}$$

$$Q - n_{\rm fs} \cdot \mathbf{T}(w) n_{\rm fs} = -\psi \quad on \ \Sigma_{\rm c} \tag{5.45}$$

$$-P_{\tau}(\mathbf{T}(w)n_{\mathrm{fs}}) - \frac{\beta\mu}{\sqrt{\kappa}}P_{\tau}w = \rho(u \wedge w) \quad on \ \Sigma_{\mathrm{c}}, \tag{5.46}$$

$$w \cdot n_{\rm sf} + \frac{\kappa}{\mu} \frac{\partial \psi}{\partial n_{\rm ef}} = 0 \quad on \ \Sigma_{\rm c}, \tag{5.47}$$

$$-\frac{\kappa}{\mu} \frac{\partial \psi}{\partial n_r} = 0 \quad on \ \Sigma_r, \tag{5.48}$$

where $C^*: \mathbb{R}^m \to (L^2(\Omega_f))^3$ is the L^2 -adjoint operator of C.

The detailed derivation is presented in appendix A. The following result on the well-posedness of the adjoint system can be easily established using the similar procedures as in the proof of lemma 5.1.

Theorem 5.2. For $u \in V_0^1(\Omega_f)$ and $\kappa \in \mathbb{K}$, there exists a unique solution $(w, \psi) \in V_0^1(\Omega_f) \times H^1(\Omega_s)$ to the adjoint system (5.39)–(5.48).

In addition, one can easily verify the following relation between the linearized state equations (5.2)–(5.10) and the adjoint equations (5.39)–(5.48), that is, for (v, z), $(w, \psi) \in V$,

$$\begin{split} 0 &= (\rho(v \cdot \nabla u + u \cdot \nabla v), w)_{\Omega_{\mathrm{f}}} + \left(\nabla \tilde{p} - \nabla \cdot (\mu(\nabla v + (\nabla v)^{T}), w)_{\Omega_{\mathrm{f}}} \right. \\ &+ \left. \left(-\nabla \cdot \left(\frac{1}{\mu} h \nabla \phi\right), \psi\right)_{\Omega_{\mathrm{s}}} + \left(-\nabla \cdot \left(\frac{\kappa}{\mu} \nabla z\right), \psi\right)_{\Omega_{\mathrm{s}}} \\ &= \rho(v, (\nabla u)^{T} w)_{\Omega_{\mathrm{f}}} - \rho(v, u \cdot \nabla w)_{\Omega_{\mathrm{f}}} + \left(v, \nabla Q - \nabla \cdot (\mu(\nabla w + (\nabla w)^{T}))_{\Omega_{\mathrm{f}}} \right. \\ &+ \left. \int_{\Sigma_{\mathrm{c}}} \left(-\frac{\beta \mu}{2\kappa^{3/2}} h\right) (P_{\tau} u) \cdot (P_{\tau} w) \mathrm{d}x + \left(\frac{1}{\mu} h \nabla \phi, \nabla \psi\right)_{\Omega_{\mathrm{s}}} + \left(z, -\nabla \cdot \left(\frac{\kappa}{\mu} \nabla \psi\right)\right)_{\Omega_{\mathrm{s}}} \\ &= \left(v, \mathcal{C}^{*}(\mathcal{C}u - \vec{y}_{\mathrm{ref}})\right)_{\Omega_{\mathrm{f}}} - \int_{\Sigma_{\mathrm{c}}} \left(\frac{\beta \mu}{2\kappa^{3/2}} h\right) (P_{\tau} u) \cdot (P_{\tau} w) \mathrm{d}x + \left(\frac{1}{\mu} h \nabla \phi, \nabla \psi\right)_{\Omega_{\mathrm{s}}}, \end{split}$$

which indicates that

$$(v, \mathcal{C}^*(\mathcal{C}u - \vec{y}_{ref}))_{\Omega_f} = \int_{\Sigma_c} \left(\frac{\beta \mu}{2\kappa^{3/2}} h \right) (P_{\tau}u) \cdot (P_{\tau}w) dx - \left(\frac{1}{\mu} h \nabla \phi, \nabla \psi \right)_{\Omega_s}.$$
 (5.49)

More detailed proof is given by (A.22) and (A.23) in appendix A.

With the knowledge of the adjoint system at our disposal, we are now ready to derive the first-order optimality conditions for solving the optimal solution to problem (P).

Theorem 5.3. *If* $\kappa^* \in \mathbb{K}$ *is the optimal solution to problem* (P), *then* κ^* *satisfies the following variational inequality*

$$J'(\kappa^*) \cdot (\kappa - \kappa^*)$$

$$= \int_{\Sigma_c} \frac{\beta \mu}{2\kappa^{*3/2}} (\kappa - \kappa^*) (P_\tau u^*) \cdot (P_\tau w^*) dx - \left(\frac{1}{\mu} (\kappa - \kappa^*) \nabla \phi^*, \nabla \psi^*\right)_{\Omega_s}$$

$$+ \alpha (\kappa^*, \kappa - \kappa^*)_{\Omega_s} + \alpha (\nabla \kappa^*, \nabla (\kappa - \kappa^*))_{\Omega_s} \geqslant 0, \quad \forall \ \kappa \in \mathbb{K},$$
 (5.50)

where (u^*, ϕ^*) and (w^*, ψ^*) are the state and adjoint state vectors associated with k^* , satisfying the state equations (2.1)–(2.12) and the adjoint equations (5.39)–(5.48), respectively.

Proof. If $\kappa^* \in X$ is the optimal solution to problem (P) and (u^*, ϕ^*) and (w^*, ψ^*) are the corresponding state and adjoint state vectors, then by (4.1) and (5.1) the following variational inequality holds

$$J'(\kappa^*) \cdot (\kappa - \kappa^*) = (\mathcal{C}^*(\mathcal{C}u^* - \vec{y}_{ref}), u^{*'}) \cdot (\kappa - \kappa^*) \Big)_{\Omega_f}$$

+ $\alpha(\kappa^*, \kappa - \kappa^*)_{\Omega_s} + \alpha(\nabla \kappa^*, \nabla(\kappa - \kappa^*))_{\Omega_s} \geqslant 0,$ (5.51)

for any $\kappa \in \mathbb{K}$. Moreover, with the help of (5.49) we get

$$\left(\mathcal{C}^*(\mathcal{C}u^* - \vec{y}_{ref}), u^{*\prime} \cdot (\kappa - \kappa^*)\right)_{\Omega_f} = \int_{\Sigma_c} \frac{\beta \mu}{2\kappa^{*3/2}} (\kappa - \kappa^*) (P_\tau u^*) \cdot (P_\tau w^*) dx - \left(\frac{1}{\mu} (\kappa - \kappa^*) \nabla \phi^*, \nabla \psi^*\right)_{\Omega_s}.$$
(5.52)

Combining (5.51) with (5.52) yields (5.50), which completes the proof.

As shown in theorem 5.3, the optimality condition (5.50) together with the state equations (2.1)–(2.12) and the adjoint equations (5.39)–(5.48) are highly nonlinear and strongly coupled. For the sake of real-life applications as well as numerical implementation, it is more realistic to approximate the permeability by functions of finite dimension. To be specific, we assume that the permeability is a weighted summation of regular functions. In other words, we let

$$\kappa = \sum_{i=1}^{M} k_i b_i,\tag{5.53}$$

where $\{b_1, b_2, \ldots, b_M\} \subset H^1(\Omega_s) \cap L^\infty(\Omega_s)$ is chosen such that it forms a basis of a finite dimensional Hilbert space $H_M = \operatorname{span}\{b_i\}_{i=1}^M$ equipped with H^1 -norm. The coefficients $k_i \in \mathbb{R}$, $i=1,2,\ldots,M$, are the weight parameters to be determined through optimization. Let $\vec{k}=[k_1,\ldots,k_M]^\mathsf{T}$, $\vec{b}=[b_1,b_2,\ldots,b_M]^\mathsf{T}$, $B_0=[(b_i,b_j)]_{i,j=1,2,\ldots,M}$, and $B_1=[(\nabla b_i,\nabla b_j)]_{i,j=1,2,\ldots,M}$. Note that both $B_0>0$ and $B_1>0$ are positive definite matrices. Then problem (P) can be reformulated as

$$\min_{\vec{k} \in \mathbb{K}_{M}} J(\vec{k}) = \min_{\vec{k} \in \mathbb{K}_{M}} \left(\frac{1}{2} \| \mathcal{C}u - y_{\text{ref}} \|_{\mathcal{Y}}^{2} + \frac{\alpha}{2} \vec{k}^{\text{T}} (B_{0} + B_{1}) \vec{k} \right), \tag{5.54}$$

where $\mathbb{K}_M = \{\vec{k} \in \mathbb{R}^M : \kappa_l \leqslant \kappa = \vec{k}^T \vec{b} \leqslant \kappa_u\}$. In this case, the optimality condition (5.1) can be interpreted more explicitly as in (e.g.[64, lemma 2.26 and theorem 2.27], [25, lemma 1.12]) from the variational inequality involving box constraints as stated in corollaries 5.3 and 5.4.

Corollary 5.3. If $\kappa^* = \sum_{i=1}^M k_i^* b_i$ is an optimal solution to problem (5.54), then it satisfies

$$\kappa^* = \min\{\kappa_u, \max\{\kappa_l, \tilde{\kappa}\}\},\tag{5.55}$$

for almost every $x \in \Omega_s$, where $\tilde{\kappa} = \sum_{i=1}^M \tilde{k}_i b_i$ satisfies the following optimality conditions

$$\int_{\Sigma_{c}} \frac{\beta \mu}{2\tilde{\kappa}^{3/2}} b_{j}(P_{\tau}u^{*}) \cdot (P_{\tau}w^{*}) dx - \left(\frac{1}{\mu} b_{j} \nabla \phi^{*}, \nabla \psi^{*}\right)_{\Omega_{s}} + \alpha \sum_{i=1}^{M} \tilde{k}_{i}(b_{i}, b_{j})_{\Omega_{s}} + \alpha \sum_{i=1}^{M} \tilde{k}_{i}(\nabla b_{i}, \nabla b_{j})_{\Omega_{s}} = 0,$$
(5.56)

for j = 1, 2, ..., M, where (u^*, ϕ^*) and (w^*, ψ^*) are the state and adjoint state vectors associated with κ^* , satisfying the state equations (2.1)–(2.12) and the adjoint equations (5.39)–(5.48), respectively.

Corollary 5.4. If κ^* is a constant, then the set of admissible functions is reduced to the interval $\mathbb{K} = [\kappa_l, \kappa_u] \subset \mathbb{R}$. The optimal solution κ^* is defined by

$$\kappa^* = \min\{\kappa_u, \max\{\kappa_l, \tilde{k}\}\},\tag{5.57}$$

where $\tilde{\kappa}$ satisfies

$$\frac{1}{2\tilde{\kappa}^{3/2}} \int_{\Sigma_{c}} \beta \mu(P_{\tau}u^{*}) \cdot (P_{\tau}w^{*}) dx - \left(\frac{1}{\mu} \nabla \phi^{*}, \nabla \psi^{*}\right)_{\Omega_{s}} + \alpha \tilde{\kappa} = 0, \tag{5.58}$$

were (u^*, ϕ^*) and (w^*, ψ^*) are the state and adjoint state vectors associated with k^* , satisfying the state equations (2.1)–(2.12) and the adjoint equations (5.39)–(5.48), respectively. Moreover, there exists at most one optimal solution $\kappa^* \in \mathbb{K}$ if α is sufficiently large.

Since the function $f(\tilde{k}) = \frac{1}{2\tilde{k}^{3/2}} \int_{\Sigma_c} \beta \mu(P_\tau u^*) \cdot (P_\tau w^*) \mathrm{d}x - \left(\frac{1}{\mu} \nabla \phi^*, \nabla \psi^*\right)_{\Omega_s} + \alpha \tilde{k}$ has at least one zero and it is monotonously increasing if $\alpha > \max\{0, \frac{3}{4}\kappa_u^{-5/2}\int_{\Sigma_c} \beta \mu(P_\tau u^*) \cdot (P_\tau w^*) \mathrm{d}x\}$, the uniqueness of the optimal solution follows immediately.

Note that the Gâteaux derivative of the cost functional $J'(\vec{k})$ is a linear functional on H_M which is a Hilbert space equipped with $H^1(\Omega_s)$ -norm, thus $DJ(\kappa) \in H_M$ can be treated as the Riesz representation of $J'(\kappa)$ (e.g. [25, p 67]) in our numerical implementation. Therefore, $DJ(\kappa)$ can be expressed as a linear combination of b_j 's and this leads to the following form

$$DJ(\kappa) := \sum_{i=1}^{M} (DJ(\kappa))_i b_i, \tag{5.59}$$

where $(DJ(\kappa))_i$ stands for the coefficient of $DJ(\kappa)$ associated with the basis function b_j . Using (5.56), we can obtain the following linear system

$$\langle DJ(\kappa), b_j \rangle_{H'_M, H_M} = \sum_{i=1}^M (DJ(\kappa))_i (b_i, b_j)_{L^2(\Omega_s)}$$

$$= \int_{\Sigma_c} \frac{\beta \mu}{2\kappa^{3/2}} b_j (P_\tau u^*) \cdot (P_\tau w^*) dx - \left(\frac{1}{\mu} b_j \nabla \phi^*, \nabla \psi^*\right)_{\Omega_s}$$

$$+ \alpha(\kappa, b_j)_{\Omega_s} + \alpha(\nabla \kappa, \nabla b_j)_{\Omega_s}, \quad j = 1, \dots, M. \quad (5.60)$$

Let η_j denote the right-hand side of (5.60), $\vec{\eta} = [\eta_1, \dots, \eta_M]^T$, and $\vec{g} = [(DJ(\kappa))_1, \dots, (DJ(\kappa))_M]^T$. Then system (5.60) is reduced to $B_0\vec{g} = \vec{\eta}$, and thus

$$\vec{g} = B_0^{-1} \vec{\eta},\tag{5.61}$$

where B_0^{-1} can be computed beforehand.

In the next section, we shall construct a gradient decent based algorithm to implement the optimality conditions numerically.

6. Numerical simulation and experimental results

In this section, an iterative optimization algorithm is constructed to identify the permeability utilizing the gradient decent method and corollary 5.3. The objective of this section is to identify the permeability of a porous micro-structure in a microfluidic chip. The algorithm is first examined in a numerical example simulating the flow dynamics around a surrogate with a uniformly distributed permeability coefficient a 3D micro-fluidic channel. The surrogate is a spherical porous structure attached in the middle of the channel and to the ceiling.

Next we construct the gradient decent based algorithm for solving the permeability κ of form (5.53). Given a set of basis functions $\{b_1, b_2, \dots, b_M\} \subset H^1(\Omega_s) \cap L^{\infty}(\Omega_s)$, the iterative gradient descent algorithm is summarized as follows.

- Step 1: for i=0, set the initial vector $\vec{k}^{(0)} = [k_1^{(0)}, \dots, k_M^{(0)}]^{\mathrm{T}}$ such that $0.5 \times 10^{-14} \leqslant \kappa^{(0)} = \vec{k}^{(0)^{\mathrm{T}}} \vec{b} \leqslant 1$ and compute the derivative $DJ(\kappa^{(i)})$ using (5.59) and (5.61) for $\kappa = \kappa^{(0)}$. Define the descent direction $V^{(0)} = -(1+\gamma)J(\kappa^{(0)})^{\gamma}DJ(\kappa^{(0)})$ for $\gamma > 0$. Also define a forgetting factor $\alpha_{\mathrm{f}} > 0$ and learning rate $\lambda^{(i)}$ ($\lambda^{(0)} = 1$).
- Step 2: choose the parameter $\alpha^{(0)} > 0$ such that $k_j^{(0)}$ and $\alpha^{(0)}V_j^{(0)}$, j = 1, 2, ..., M, have the same order of magnitude, where $V_j^{(i)}$ is the jth coefficients of $V^{(i)}$ represented by the basis functions in the Hilbert space H_M . Compute the new parameter $\kappa^{(i+1)} = \min\{1, \max\{0.5 \times 10^{-14}, \kappa^{(i)} + \alpha^{(i)}V^{(i)}\}\}$.
- Step 3: for i>0, compute the derivative $DJ(\kappa^{(i)})$ using (5.59) and (5.61) for $\kappa=\kappa^{(i)}$ and choose the parameter $\alpha^{(i)}>0$ such that $(1+\gamma)\alpha^{(i)}J(\kappa^{(i)})^{\gamma}|DJ(\kappa^{(i)})|\leqslant \bar{\alpha}_f|V^{(i-1)}|$ for some $\bar{\alpha}_f>0$ satisfying $\bar{\alpha}_f+\alpha_f<1$. Define the descent direction $V^{(i)}=\alpha_fV^{(i-1)}+\bar{\alpha}DJ(\kappa^{(i)})$, where $\bar{\alpha}=-(1-\alpha_f)(1+\gamma)\alpha^{(i)}J(\kappa^{(i)})^{\gamma}$.
- Step 4: readjust $\lambda^{(i)}$ such that $\lambda^{(i)} < \lambda^{(i-1)}$.
- Step 5: if $\|\kappa^{(i+1)} \kappa^{(i)}\|/\|\kappa^{(i)}\| \le \epsilon_{\text{stop}}$ or $i > N_{\text{stop}} > 0$ stop the iteration; otherwise set $\kappa^{(i+1)} = \min\{1, \max\{0.5 \times 10^{-14}, \kappa^{(i)} + \lambda^{(i)}V^{(i)}\}\}$ and redefine $V^{(i)} = (\kappa^{(i+1)} \kappa^{(i)})/\lambda^{(i)}$ and go to step 3.

The algorithm is designed such that it provides fast convergence with linear rate. At each step we calculate the descent direction as the weighted summation of two terms: the first term is borrowed from the previous descent direction and the second term $(1 + \gamma)\alpha^{(i)}J(\kappa^{(i)})^{\gamma}DJ(\kappa^{(i)})$ is proportional to the Gâteaux derivative. The parameter $(1 + \gamma)J(\kappa^{(i)})^{\gamma}$ adjusts the magnitude of

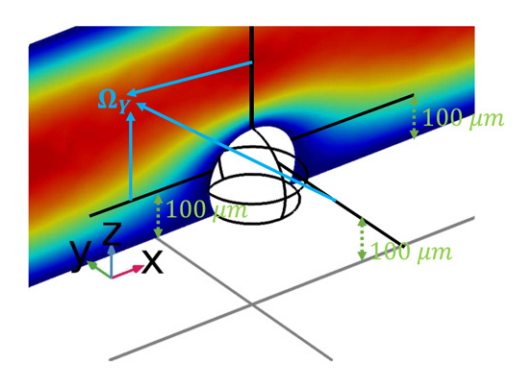


Figure 2. The measurement space composed of three perpendicular lines, two horizontal lines $100 \ \mu m$ above xy-plane and the third line along z-axis.

the second term according to the observation error, and $\alpha^{(i)}$ and $\alpha_{\rm f}$ are chosen to ensure that the norm of descent direction reduces in time. $\lambda^{(i)}$ is adjusted to compensate for the chattering near optimal solution. We pick this parameter or learning rate to get smaller by a factor whenever chattering occurs. Finally, $\alpha^{(0)}$ is set such that the maximum move towards optimal solution happens at the initial step.

For this choice of parameters, it can be shown that the projected gradient algorithm above follows a linear convergence rate. However, the proof is not within the scope of this paper and will be addressed in our future work on numerical study of this problem.

In order to check validity of the algorithm, we tested a similar numerical phantom in which the permeability is assumed to be constant. The optimality conditions are addressed in corollary 5.4. For this constant permeability estimation experiment, we have set the regularization term to zero in the cost functional. Although for more complex and spatial dependent permeability identification, the regularization parameter can be treated as a hyperparameter (optimization parameters) and adjusted depending on the experimental set-up. These parameters are selected by trial and error to increase the convergence rate.

In the current work, the flow equations and its adjoint problem were solved using FEM in COMSOL. For this purpose, the weak representation of the system and linear base functions over tetrahedral elements were utilized to approximate the system with a finite-dimensional one. In this setting, the conservation equation is treated as a separate equation and both velocity and pressure are obtained from solving a coupled set of nonlinear algebraic equations. An example of FEM application for Navier–Stokes equations can be found in [21]. We have used COMSOL 3.5 to solve the flow and adjoint equations via MATLAB livelink iteratively, without explicitly calculating the matrix form algebraic equations, where we used a fine mesh around the spherical structure and a coarse mesh away from this structure.

For the experimental tests, we implemented the algorithm in an experimental set-up with a 3D printed porous scaffold of different pore sizes in the microfluidic channel. The permeability of the surrogates is estimated using the velocity measurements along three perpendicular lines (figure 2). These lines are numerically shown to have maximum sensitivity to permeability variation.

6.1. Numerical example

We first examine the performance of the iterative optimization algorithm in a numerical example resembling the surrogate micro-environment. Since the upper bound of permeability never reaches 1, we set $\kappa_u = 1 \text{ m}^2$. On the other hand, for $\kappa < 0.5 \times 10^{-14} \text{ m}^2$, the flow

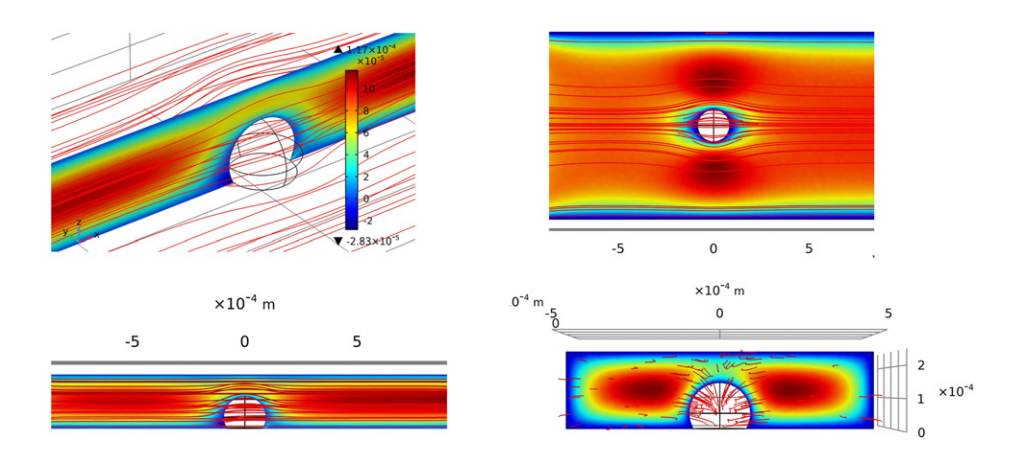


Figure 3. Velocity solution in flow direction at three different planes.

dynamics around the surrogate will not experience any variation subject to small perturbations of the permeability of the same order of magnitude. Thus we set $\kappa_l = 0.5 \times 10^{-14} \text{ m}^2$. The flow equations were solved for a known constant permeability coefficient. Here, in the reference model the permeability is $\kappa = 1.88 \times 10^{-13} \text{ m}^2$ and the slip rate coefficient is $\beta = 0.1$. The system's response was augmented with white noise and used as experimental data. Next, the synthesized experimental data was utilized to reconstruct the permeability via a recursive gradient based technique.

A 2D cross section of the 3D channel used in the numerical simulations is shown in figure 1. The channel dimensions are $4\times25\times0.25$ mm. The porous structure is assumed to be spherical of radius 50 μ m and its protrusion inside the channel is 150 μ m. Furthermore, the velocity at the channel input Σ_i is $U_0 = 6.6\times10^{-5}$ m s⁻¹, the input flow source at Σ_r is $q_0(x) = 2\times10^{-5}$ m s⁻¹, and we have used the mechanical properties of the water. The slip rate coefficient β was chosen according to the values reported in [9] given the range of porosity and permeability coefficient ($\beta = 0.1$).

In permeability identification of the porous surrogate, $\lambda_0=1$ and $\lambda_{i+1}=\lambda_i/2$ whenever $(V_i,V_{i+1})_{\Omega_s}\leqslant 0$. In order to choose the parameter α_i satisfying condition of step 3, we set $\alpha_i=10$ and keep dividing by $a_0=1.1$ such that $\bar{\alpha}_f+\alpha_f<1$ and $\bar{\alpha}_f DJ(\kappa_i)< V_{i-1}$. Other parameters of the iterative algorithm are $\gamma=1$ and $\alpha_f=0.2$. These parameters are chosen by trial and error to increase the convergence rate.

At each iteration, the system was solved for updated parameter and the solution was used to solve the adjoint problem. Moreover, the solution of the adjoint problem was utilized to define the gradient vector. The velocity profiles around the porous micro-structure for $\kappa=1.88\times 10^{-13}~\text{m}^2$ at different cross-sections are shown in figure 3. We have solved the optimization problem for two different initial conditions $\kappa=1.88\times 10^{-7}~\text{m}^2$ and $\kappa=1.88\times 10^{-9}~\text{m}^2$. The initial guess is selected based on the range of identifiability of the permeability, that is, $\kappa\geqslant 0.5\times 10^{-14}~\text{m}^2$. For $\kappa<0.5\times 10^{-14}~\text{m}^2$, the flow dynamics around the surrogate will not experience any variation subject to small perturbations of the permeability of the same order. Therefore, we know that the initial guess must be larger that this value. To this end, we chose the initial guess to be five and seven order of magnitude larger than the minimum value. In microfluidic chip, larger permeability values lead to less sensitivity in the velocity profile as a function of permeability and thus uncertainty in the identification process.

The convergence of the permeability and its corresponding output error convergence are depicted in figure 4. The sampled measurement defined by (2.14) over the subdomain

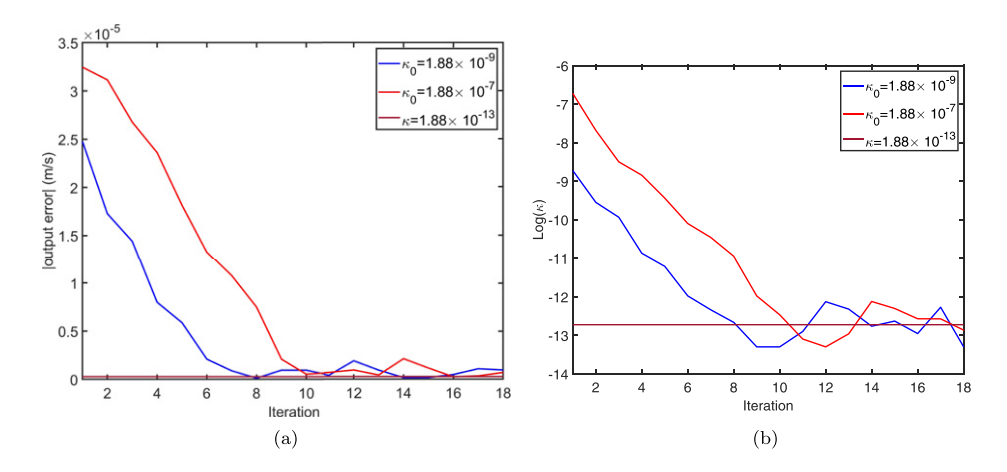


Figure 4. Convergence of the output error L^2 -norm over measurement space (a) and convergence of the permeability to $\kappa=1.88\times10^{-13}$ (b) at different consecutive iteration.

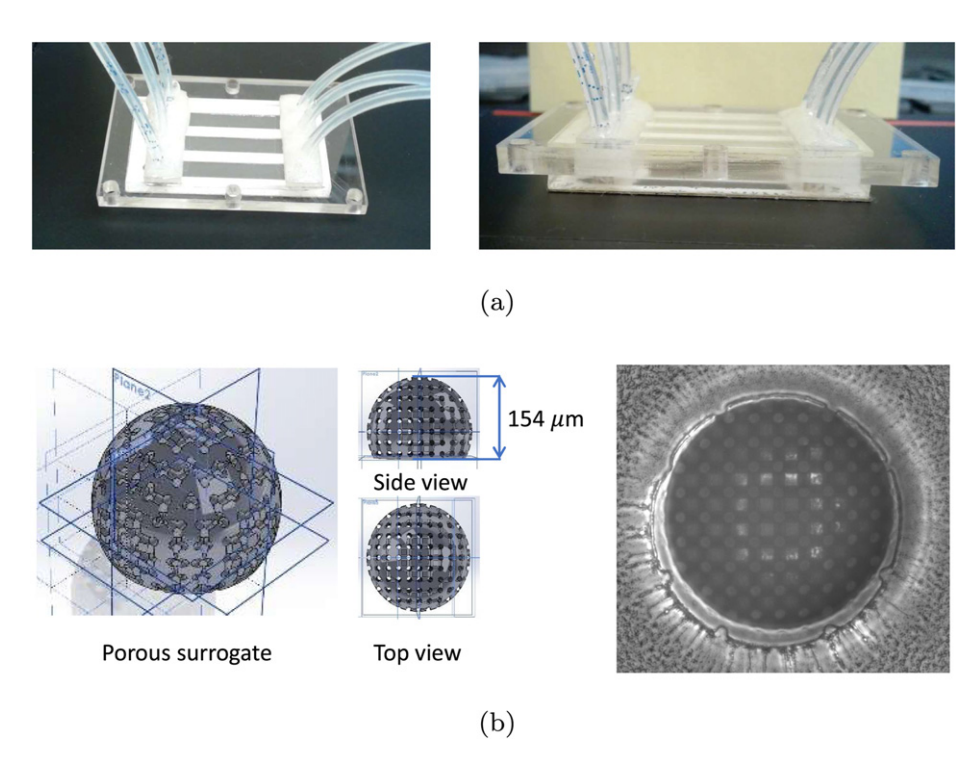


Figure 5. 3D structure of the fluidic chip (a) and 3D printed porous surrogate (b) used in *in vitro* experiments.

 $\Omega_Y = \bigcup_{i=1}^m \overline{\Omega}_i$ shown in figure 2 where the measurement sets Ω_i span across three perpendicular lines. It is evident from these figures that the permeability coefficient can be recovered in a few iterations less than 10.

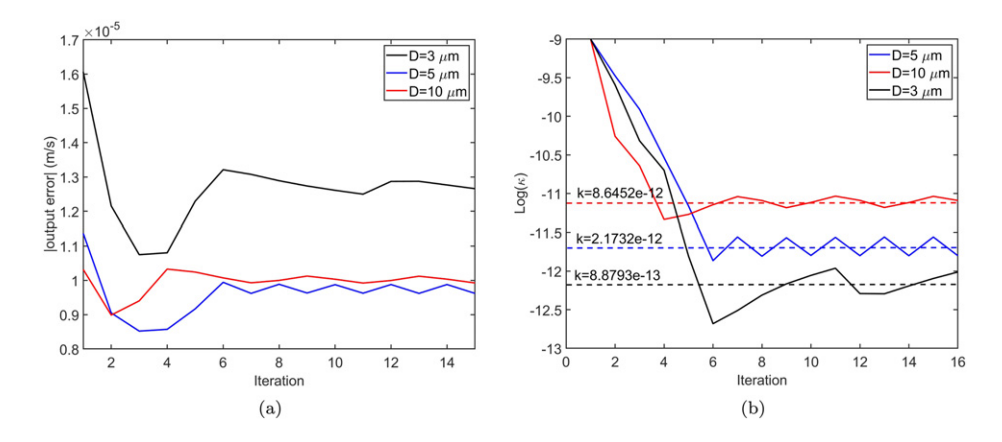


Figure 6. Convergence of output error L^2 -norm over the measurement space (a) and convergence of permeability estimate (b) for three different pore sizes for the porous structure shown in figure 5.

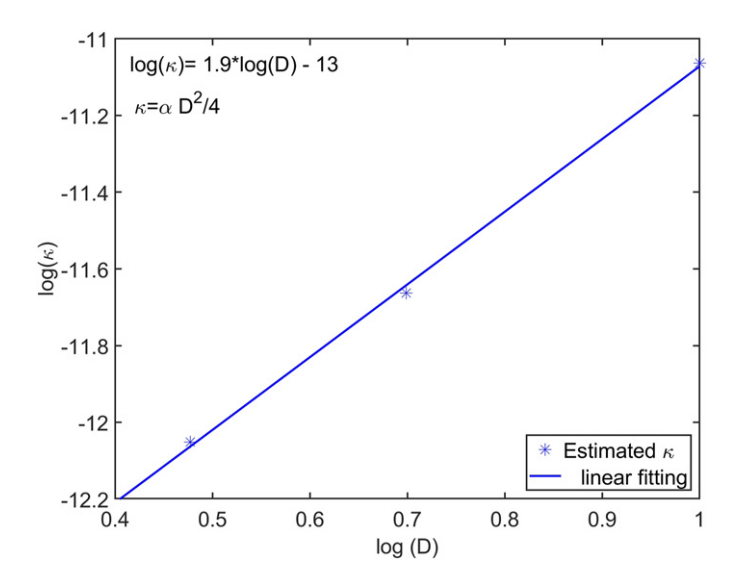


Figure 7. Log-log plot of the permeability estimate as a function of pore size for three different pore sizes for the structure shown in figure 5.

6.2. Experimental validation

Next, the proposed optimization based approach was implemented in the estimation of the permeability of a 3D printed porous scaffold on a fluidic chip experimentally. The width of the chip was downsized from 4 mm to increase the velocity around the porous surrogate. The porous surrogate of 200 μ m diameter is printed using Nanoscribe 3D printing (Nanoscribe's 3D laser lithography system, Photonic Professional GT) to the floor of the microchannel. The protrusion depth is 50 μ m. The porous structure is designed by excluding a 3D scaffold from a solid sphere (figure 5(b)) with three different pore sizes (3, 5, and 10 μ m in diameter). For this structure, the permeability satisfies

$$\kappa \propto \frac{D^2}{4},$$
 (6.1)

where D denotes the pores diameter.

We propose to use optical observations to measure the flow velocity field around the 3D printed surrogate, where the velocity field is then utilized to estimate the surrogate permeability. The velocity field was measured using a well-established particle image velocimetry (PIV) technique [2, 69]. The micro PIV technique was adjusted to match the requirements of the experimental velocity measurement. The optical measurement was performed via an inverted laser scanning confocal microscope (Olympus FV1000). A flow of 2 μ l min⁻¹ containing fluorescent particle tracers of density of 30 μ l of fluorescent in 1 ml of saline enters the channel. The tracers were Sky Blue nano-particles (excitation/emission 660/700 nm, 1% w/v, FH-2070-2, Spherotech, Lake Forest IL) of size 500–800 nm. The flow was infused constantly using a syringe pump. The position of the particles was recorded using the confocal microscope with two different objectives, $40 \times$ and $20 \times$, to image particles 500 and 800 nm in size, respectively depending on the field on imaging. Images were acquired at 2 μ s/pixel dwell time and 256 \times 256 pixel resolution. Imaging was carried out at different z-planes.

The velocity profile measurement along the subspace exhibited in figure 3 was used in the numerical estimation of permeability of the porous scaffolds. The convergence of the permeability estimates is depicted in figure 6 for three different pore sizes. This figure indicates the convergence of the permeability to constant values. In figure 7, we plotted the permeability estimate as a function of pores diameter in a log-log plot. The linear fitted curve to the estimated point reveals that the estimated permeability follows the theoretical prediction defined by (6.1).

7. Conclusion and discussion

In this work, we studied the problem of distributed permeability identification of a porous structure, which plays a critical role in drug delivery and cancer treatment. We proposed a numerical and experimental tool to measure this property of a porous surrogate of tumor nodule on a microfluidic chip. For this purpose, the flow velocity field around the surrogate, represented by coupled Navier–Stokes–Darcy equations, was used as a tracer for the permeability. An optimization problem was solved to estimate the permeability such that the regularized L^2 -norm of the difference between the system's solution for the external velocity field and its measurement is minimized.

It was shown both numerically and experimentally that the permeability of a porous scaffold with homogeneous porosity can be estimated from velocity field measurement. Scaffolds with three different pore sizes were tested experimentally, and the permeability up to order 10^{-14} m² was shown to be identifiable from the optical velocity field measurement of order $0.5 \, \mu \text{m s}^{-1}$. Moreover, the experimental estimated permeability was shown to follow a semi-empirical relation exhibiting that the permeability is correlated with the squared diameter of the pore size, as proved in the literature for the chosen scaffold [15].

We have tested the permeability of a homogeneous porous media printed in a microfluidic chip via Nanoscribe micro-scale 3D printing technology. Estimation of permeability of an inhomogeneous porous surrogate with less regularity properties will be considered in future. It is worth to point out that the proposed theoretical approach supports inhomogeneous porosity estimation. The experimental design can be adjusted to measure such inhomogeneous permeability with a degree of regularity on a chip. We will also consider adding interstitial flow

source to the surrogate which will increase the sensitivity of the measured velocity field and the estimation precision, as well as the range of measurable permeability coefficient.

In our numerical and experimental design, the velocity field was measured over a predefined subset. Specifically, the measurement subset was chosen such that the sensitivity to unknown parameters is maximized based on numerical solution of the system and a sensitivity analysis. However, prior knowledge on the optimal sensors locations will provide a better guidance to increase the estimation efficiency, and this will be further investigated in our future work.

Finally, our proposed approach can be easily adjusted to different applications and more general environment. It imposes minimal experimental restrictions on the surrogate microenvironment and can be potentially extended for *in vivo* permeability estimation.

Acknowledgments

S Afshar would like to acknowledge Dr Walfre Franco for his financial and intellectual support in designing and implementing the experimental set-up for this work. W Hu was partially supported by the NSF Grants DMS-2005696 and DMS-2111486. The authors also acknowledge Kris Carlson and Dr Jeffrey E Arle at Harvard Medical School/Mount Auburn Hospital, Massachusetts, for providing the COMSOL license.

Data availability statement

The data that support the findings of this study are available upon reasonable request from the authors.

Appendix A

A.1. Proof of lemma 3.1

Proof. It is straightforward to show that $\bar{a}(\cdot, \cdot)$ is continuous and coercive by using Poincaré and Korn's inequalities together with trace theorem. We first show the continuity of this bilinear form. Note that

$$\left| \frac{1}{2\mu} \int_{\Omega_{\mathbf{f}}} \mathbf{T}(u) \cdot \mathbf{T}(w) dx \right| \leqslant C \frac{1}{2\mu} \|u\|_{H^{1}(\Omega_{\mathbf{f}})} \|w\|_{H^{1}(\Omega_{\mathbf{f}})},$$

$$\left| \int_{\Omega_{\mathbf{s}}} \frac{\kappa}{\mu} \nabla \phi \cdot \nabla \psi dx \right| \leqslant C \frac{\kappa}{\mu} \|\phi\|_{H^{1}(\Omega_{\mathbf{s}})} \|\psi\|_{H^{1}(\Omega_{\mathbf{s}})},$$

$$\left| \int_{\Sigma_{\mathbf{c}}} \phi(w \cdot n_{\mathbf{f}\mathbf{s}}) dx \right| \leqslant \|\phi\|_{L^{2}(\Sigma_{\mathbf{c}})} \|w\|_{L^{2}(\Sigma_{\mathbf{c}})} \leqslant C \|\phi\|_{H^{1}(\Omega_{\mathbf{s}})} \|w\|_{H^{1}(\Omega_{\mathbf{f}})}.$$

Similarly,

$$\left| \int_{\Sigma_{c}} (u \cdot n_{sf}) \psi dx \right| \leqslant C \|u\|_{H^{1}(\Omega_{f})} \|\psi\|_{H^{1}(\Omega_{s})}$$

and

$$\left| \int_{\Sigma_{\mathsf{c}}} \frac{\beta \mu}{\sqrt{\kappa}} (P_{\tau} u) \cdot (P_{\tau} w) \mathrm{d}x \right| \leqslant C \frac{\beta \mu}{\sqrt{\kappa_{l}}} \|u\|_{H^{1}(\Omega_{\mathsf{f}})} \|w\|_{H^{1}(\Omega_{\mathsf{f}})}.$$

Therefore,

$$|\bar{a}((u,\phi);(w,\psi))| \leqslant C_{\bar{a}} \left(\|u\|_{H^{1}(\Omega_{f})} + \|\phi\|_{H^{1}(\Omega_{s})} \right) \left(\|w\|_{H^{1}(\Omega_{f})} + \|\psi\|_{H^{1}(\Omega_{s})} \right),$$
(A.1)

for some $C_{\bar{a}} > 0$.

To see the coercivity of $\bar{a}(\cdot, \cdot)$, by (3.5) we have

$$\bar{a}((u,\phi);(u,\phi)) = \frac{1}{2\mu} \int_{\Omega_{\mathbf{f}}} \mathbf{T}(u) \cdot \mathbf{T}(u) dx + \int_{\Sigma_{\mathbf{c}}} \frac{\beta \mu}{\sqrt{\kappa}} (P_{\tau}u) \cdot (P_{\tau}u) dx
+ \int_{\Omega_{\mathbf{s}}} \frac{\kappa}{\mu} \nabla \phi \cdot \nabla \phi dx
\geqslant \frac{C_{1}}{2\mu} \|u\|_{H^{1}(\Omega_{\mathbf{f}})}^{2} + \frac{C_{2}\kappa_{l}}{\mu} \|\phi\|_{H^{1}(\Omega_{\mathbf{s}})}
\geqslant \alpha_{0}(\|u\|_{H^{1}(\Omega_{\mathbf{f}})}^{2} + \|\phi\|_{H^{1}(\Omega_{\mathbf{s}})}^{2}), \tag{A.2}$$

where the constants $C_1, C_2 > 0$ only depend on the domain Ω_f and $\alpha_0 = \min\{\frac{C_1}{2\mu}, \frac{C_2\kappa_l}{\mu}\} > 0$, and thus the coercivity follows.

A.2. Proof of theorem 3.1

Proof. The proof of existence follows as in that of [63, theorem 1.5], [20, theorem 2.3, chapter IV] and [13, theorem 2.1, chapter 2]. We first show that there exists some constant $C_0 > 0$ such that

$$\bar{a}((\bar{u},\phi);(\bar{u},\phi)) + \bar{b}(\bar{u},\tilde{u},\bar{u}) + \bar{b}(\tilde{u},\bar{u},\bar{u}) + \bar{b}(\bar{u},\bar{u},\bar{u}) \geqslant C_0(\|\bar{u}\|_{H^1(\Omega_t)}^2 + \|\phi\|_{H^1(\Omega_t)}^2),$$

or due to (3.9)

$$\bar{a}((\bar{u},\phi);(\bar{u},\phi)) + \bar{b}(\bar{u},\tilde{u},\bar{u}) \geqslant C_0(\|\bar{u}\|_{H^1(\Omega_c)}^2 + \|\phi\|_{H^1(\Omega_c)}^2). \tag{A.3}$$

From lemma 3.2, we can conclude that

$$\bar{b}(\bar{u}, \tilde{u}, \bar{u}) \leqslant \frac{\alpha_0}{2} \|\bar{u}\|_{H^1(\Omega_f)}^2,\tag{A.4}$$

for α_0 given by (A.2). With the help of (3.8) and (A.2) it is easy to see that

$$\begin{split} \bar{a}((\bar{u},\phi);(\bar{u},\phi)) + \bar{b}(\bar{u},\tilde{u},\bar{u}) \geqslant \alpha_0(\|\bar{u}\|_{H^1(\Omega_{\mathrm{f}})}^2 + \|\phi\|_{H^1(\Omega_{\mathrm{s}})}^2) - \frac{\alpha_0}{2} \|\bar{u}\|_{H^1(\Omega_{\mathrm{f}})}^2 \\ \geqslant \frac{\alpha_0}{2} (\|\bar{u}\|_{H^1(\Omega_{\mathrm{f}})}^2 + \|\phi\|_{H^1(\Omega_{\mathrm{s}})}^2). \end{split}$$

Letting $C_0 = \frac{\alpha_0}{2}$, then (A.3) follows. Further by the boundedness of L given by (3.10), we conclude that there exists a unique solution to (3.16) using the Lax–Milgram theorem (e.g. [72, chapter 2, section 2.3.4]).

To see the estimate (3.17), in light of (3.8), (3.10), (3.13) and (A.1), it is evident that

$$\begin{split} \bar{a}((\tilde{u},0);(\tilde{u},0)) &= \frac{1}{2\mu} \int_{\Omega_{f}} \mathbf{T}(\tilde{u}) \cdot \mathbf{T}(\tilde{u}) + \int_{\Sigma_{c}} \left(\frac{\beta\mu}{\sqrt{\kappa}} \tilde{u} \cdot \tau_{sf} \right) (\tilde{u} \cdot \tau_{sf}) dx \\ &\leqslant \frac{C}{2\mu} \|\tilde{u}\|_{H^{1}(\Omega_{f})}^{2} + \frac{\beta\mu}{\sqrt{\kappa_{l}}} \|\tilde{u}\|_{H^{1}(\Omega_{f})}^{2} \\ &\leqslant c_{0} \left(\frac{C}{2\mu} + \frac{\beta\mu}{\sqrt{\kappa_{l}}} \right) \|u_{0}\|_{H^{1/2}(\Sigma_{i})}^{2} \end{split}$$

$$L(\bar{u},\phi) \leqslant C(\|p_0\|_{L^2(\Sigma_0)}^2 + \|q_0\|_{L^2(\Sigma_\Gamma)}^2) + \frac{\alpha_0}{8} \|\bar{u}\|_{H^1(\Omega_{\mathrm{f}})}^2 + \frac{\alpha_0}{4} \|\phi\|_{H^1(\Omega_{\mathrm{s}})}^2,$$

and

$$\bar{b}(\tilde{u},\tilde{u},\bar{u}) \leqslant C_{\bar{b}}\rho \|\tilde{u}\|_{H^1(\Omega_{\mathrm{f}})}^2 \|\bar{u}\|_{H^1(\Omega_{\mathrm{f}})} \leqslant C\rho^2 \|u_0\|_{H^{1/2}(\Sigma_{\hat{\mathbf{i}}})}^4 + \frac{\alpha_0}{8} \|\bar{u}\|_{H^1(\Omega_{\mathrm{f}})}^2.$$

Therefore,

$$\begin{split} \frac{\alpha_0}{2}(\|\bar{u}\|_{H^1(\Omega_{\mathrm{f}})}^2 + \|\phi\|_{H^1(\Omega_{\mathrm{s}})}^2) &\leq c_0 \left(\frac{C}{2\mu} + \frac{\beta\mu}{\sqrt{\kappa_l}}\right) \|u_0\|_{H^{1/2}(\Sigma_{\mathrm{i}})}^2 + C \left(\|p_0\|_{L^2(\Sigma_{\mathrm{o}})}^2 + \|q_0\|_{L^2(\Sigma_{\mathrm{r}})}^2\right) + \frac{\alpha_0}{4} \|\bar{u}\|_{H^1(\Omega_{\mathrm{f}})}^2 \\ &+ \frac{\alpha_0}{4} \|\phi\|_{H^1(\Omega_{\mathrm{s}})}^2 + C\rho^2 \|u_0\|_{H^{1/2}(\Sigma_{\mathrm{i}})}^4, \end{split}$$

and hence,

$$\begin{split} \|\bar{u}\|_{H^{1}(\Omega_{f})}^{2} + \|\phi\|_{H^{1}(\Omega_{s})}^{2} &\leq \frac{4c_{0}}{\alpha_{0}} \left(\frac{C}{2\mu} + \frac{\beta\mu}{\sqrt{\kappa_{l}}}\right) \|u_{0}\|_{H^{1/2}(\Sigma_{i})}^{2} + C\frac{4}{\alpha_{0}} \left(\|p_{0}\|_{L^{2}(\Sigma_{0})}^{2} + \|q_{0}\|_{L^{2}(\Sigma_{r})}^{2}\right) + C\frac{4}{\alpha_{0}} \rho^{2} \|u_{0}\|_{H^{1/2}(\Sigma_{i})}^{4}, \end{split} \tag{A.5}$$

which establishes the estimate (3.17). Finally, (3.18) follows from (3.13)–(3.15). This completes the proof. \Box

A.3. Derivation of the adjoint system

Proof of theorem 5.1. First, using Stokes formula we know that there exits pressure Q such that

$$\int_{\Omega_f} \nabla Q \cdot v \, dx = \int_{\partial \Omega_f} (v \cdot n) Q \, dx - \int_{\Omega_f} (\nabla \cdot v) Q \, dx = \int_{\partial \Omega_f} (v \cdot n) Q \, dx. \quad (A.6)$$

Now taking the inner product of equation (5.2) with w gives

$$0 = (\rho(v \cdot \nabla u + u \cdot \nabla v), w)_{\Omega_{f}} + (\nabla \tilde{p} - \nabla \cdot (\mu(\nabla v + (\nabla v)^{T}), w)_{\Omega_{f}}$$

$$= \rho(v, (\nabla u)^{T}w)_{\Omega_{f}} + \int_{\partial\Omega_{f}} \rho(u \cdot n)(v \cdot w)dx - \rho(v, u \cdot \nabla w)_{\Omega_{f}}$$

$$+ \int_{\partial\Omega_{f}} (w \cdot n)\tilde{p} dx - \int_{\partial\Omega_{f}} \mathbf{T}(v)n \cdot w dx + \int_{\partial\Omega_{f}} \mathbf{T}(w)n \cdot v dx$$

$$- \int_{\partial\Omega_{f}} (v \cdot n)Q dx + (v, \nabla Q - \nabla \cdot (\mu(\nabla w + (\nabla w)^{T}))_{\Omega_{f}}$$

$$= \rho(v, (\nabla u)^{T}w)_{\Omega_{f}} + \int_{\Sigma_{c}} \rho(u \cdot n_{fs})(v \cdot w)dx - \rho(v, u \cdot \nabla w)_{\Omega_{f}}$$

$$+ \int_{\Sigma_{c}} z(w \cdot n_{fs})dx - \int_{\Sigma_{c}} \rho((v)^{T}u)(w \cdot n_{fs})dx$$

$$- \int_{\Sigma_{c}} P_{\tau}(\mathbf{T}(v)n_{fs}) \cdot (P_{\tau}w)dx + \int_{\Sigma_{c} \cup \Sigma_{c}} \mathbf{T}(w)n \cdot ((v \cdot n)n + P_{\tau}v) dx$$

$$- \int_{\Sigma_{c} \cup \Sigma_{c}} (v \cdot n)Q dx + (v, \nabla Q - \nabla \cdot (\mu(\nabla w + (\nabla w)^{T}))_{\Omega_{f}}. \tag{A.7}$$

From (5.13) we get

$$\int_{\Sigma_{c}} P_{\tau}(\mathbf{T}(v)n_{fs}) \cdot (P_{\tau}w) dx = -\int_{\Sigma_{c}} \left(-\frac{\beta\mu}{2\kappa^{3/2}} h P_{\tau}u + \frac{\beta\mu}{\sqrt{\kappa}} P_{\tau}v \right) \cdot (P_{\tau}w) dx.$$
(A.8)

Moreover,

$$\int_{\Sigma_{c}} \rho(u \cdot n_{fs})(v \cdot w) dx$$

$$= \rho \int_{\Sigma_{c}} (u \cdot n_{fs}) \left[(v \cdot n_{fs})(w \cdot n_{fs}) + (P_{\tau}v) \cdot (P_{\tau}w) \right] dx$$

$$= \rho \int_{\Sigma_{c}} \left[(u \cdot n_{fs})(v \cdot n_{fs})(w \cdot n_{fs}) + (u \cdot n_{fs})(P_{\tau}v) \cdot (P_{\tau}w) \right] dx$$

$$+ (P_{\tau}u) \cdot (P_{\tau}v)(w \cdot n_{fs}) - (P_{\tau}u) \cdot (P_{\tau}v)(w \cdot n_{fs}) \right] dx$$

$$= \rho \int_{\Sigma_{c}} \left[(u \cdot v)(w \cdot n_{fs}) + (u \cdot n_{fs})(P_{\tau}v) \cdot (P_{\tau}w) - (P_{\tau}u) \cdot (P_{\tau}v)(w \cdot n_{fs}) \right] dx$$

$$= \rho \int_{\Sigma_{c}} \left\{ (u \cdot v)(w \cdot n_{fs}) + \left[(u \cdot n_{fs})(P_{\tau}w) - (P_{\tau}u)(w \cdot n_{fs}) \right] \cdot (P_{\tau}v) \right\} dx$$

$$= \rho \int_{\Sigma_{c}} \left[(u \cdot v)(w \cdot n_{fs}) + (u \wedge w) \cdot (P_{\tau}v) \right] dx, \tag{A.9}$$

where the notation \wedge is defined by

$$u \wedge w = (u \cdot n_{\rm fs})(P_{\tau}w) - (P_{\tau}u)(w \cdot n_{\rm fs}).$$

Substituting (A.8) and (A.9) into (A.7) leads to

$$0 = \rho(v, (\nabla u)^{\mathrm{T}} w)_{\Omega_{\mathrm{f}}} - \rho(v, u \cdot \nabla w)_{\Omega_{\mathrm{f}}} + \rho \int_{\Sigma_{\mathrm{c}}} (u \wedge w) \cdot (P_{\tau}v) \mathrm{d}x$$

$$+ \int_{\Sigma_{\mathrm{c}}} z(w \cdot n_{\mathrm{fs}}) \mathrm{d}x + \int_{\Sigma_{\mathrm{c}}} \left(-\frac{\beta \mu}{2\kappa^{3/2}} h P_{\tau} u + \frac{\beta \mu}{\sqrt{\kappa}} P_{\tau} v \right) \cdot (P_{\tau}w) \mathrm{d}x$$

$$+ \int_{\Sigma_{\mathrm{o}}} \mathbf{T}(w) n_{\mathrm{o}} \cdot (v \cdot n_{\mathrm{o}}) n_{\mathrm{o}} \, \mathrm{d}x + \int_{\Sigma_{\mathrm{c}}} \mathbf{T}(w) n_{\mathrm{fs}} \cdot (v \cdot n_{\mathrm{fs}}) n_{\mathrm{fs}} \, \mathrm{d}x$$

$$+ \int_{\Sigma_{\mathrm{c}}} \mathbf{T}(w) n_{\mathrm{fs}} \cdot P_{\tau} v \, \mathrm{d}x - \int_{\Sigma_{\mathrm{o}}} (v \cdot n_{\mathrm{o}}) Q \, \mathrm{d}x - \int_{\Sigma_{\mathrm{c}}} (v \cdot n_{\mathrm{fs}}) Q \, \mathrm{d}x$$

$$+ \left(v, \nabla Q - \nabla \cdot \left(\mu (\nabla w + (\nabla w)^{\mathrm{T}}) \right)_{\Omega_{\mathrm{c}}} \right)$$
(A.10)

To derive the adjoint state of the porous media, we take the inner produce of (5.4) with ψ and this follows

$$\begin{split} 0 &= - \left(\nabla \cdot \left(\frac{1}{\mu} h \nabla \phi \right), \psi \right)_{\Omega_{\mathbf{S}}} - \left(\nabla \cdot \left(\frac{\kappa}{\mu} \nabla z \right), \psi \right)_{\Omega_{\mathbf{S}}} \\ &= - \int_{\Sigma_{\mathbf{C}} \cup \Sigma_{\mathbf{r}}} \frac{1}{\mu} h (\nabla \phi \cdot n) \psi \, \mathrm{d}x + \left(\frac{1}{\mu} h \nabla \phi, \nabla \psi \right)_{\Omega_{\mathbf{S}}} - \int_{\Sigma_{\mathbf{C}} \cup \Sigma_{\mathbf{r}}} \frac{\kappa}{\mu} (\nabla z \cdot n) \psi \, \mathrm{d}x \\ &+ \int_{\Sigma_{\mathbf{C}} \cup \Sigma_{\mathbf{r}}} \frac{\kappa}{\mu} (\nabla \psi \cdot n) z \, \mathrm{d}x - \left(z, \nabla \cdot \left(\frac{\kappa}{\mu} \nabla \psi \right) \right)_{\Omega_{\mathbf{S}}}, \end{split}$$

which by (5.9)-(5.11) and (5.14) yields

$$0 = -\int_{\Sigma_{c}} (v \cdot n_{fs}) \psi \, dx + \left(\frac{1}{\mu} h \nabla \phi, \nabla \psi\right)_{\Omega_{s}} + \int_{\Sigma_{c} \cup \Sigma_{c}} \frac{\kappa}{\mu} (\nabla \psi \cdot n) z \, dx - \left(z, \nabla \cdot \left(\frac{\kappa}{\mu} \nabla \psi\right)\right)_{\Omega_{s}}.$$
(A.11)

In light of (A.10) and (A.11), we first impose

$$\rho((\nabla u)^{\mathsf{T}} w - u \cdot \nabla w) + \nabla Q - \nabla \cdot (\mu(\nabla w + (\nabla w)^{\mathsf{T}})) = \mathcal{C}^*(\mathcal{C}u - \vec{\mathsf{y}}_{\mathsf{ref}}), \tag{A.12}$$

$$\nabla \cdot w = 0, \tag{A.13}$$

$$-\nabla \cdot \left(\frac{\kappa}{\mu} \nabla \psi\right) = 0. \tag{A.14}$$

To derive the boundary conditions, it is clear that

$$w = 0$$
 on $\Sigma_{\rm i}$, and $w = 0$ on $\Sigma_{\rm w}$. (A.15)

On boundary Σ_r , impose

$$-\int_{\Sigma_{\rm r}} \frac{\kappa}{\mu} (\nabla \psi \cdot n) z \, \mathrm{d}x = 0, \quad \forall \ z \in H^1(\Omega_{\rm s}),$$
or
$$-\frac{\kappa}{\mu} \nabla \phi \cdot n|_{\Sigma_{\rm r}} = 0. \tag{A.16}$$

On boundary Σ_0 , impose

$$-\int_{\Sigma_{0}} \mathbf{T}(w) n_{o} \cdot (v \cdot n_{o}) n_{o} \, \mathrm{d}x + \int_{\Sigma_{0}} (v \cdot n_{o}) Q \, \mathrm{d}x = 0, \quad \forall \ v \in V_{0}^{1}(\Omega_{\mathrm{f}}),$$
or $Q - n_{o} \cdot \mathbf{T}(w) n_{o} = 0$ on Σ_{o} , (A.17)

and

$$w \times n_0 = 0$$
 on Σ_0 . (A.18)

Moreover, on boundary Σ_c we let

$$\rho \int_{\Sigma_{c}} (u \wedge w) \cdot (P_{\tau}v) dx + \int_{\Sigma_{c}} z(w \cdot n_{fs}) dx + \int_{\Sigma_{c}} \frac{\beta \mu}{\sqrt{\kappa}} (P_{\tau}v) \cdot (P_{\tau}w) dx
+ \int_{\Sigma_{c}} \mathbf{T}(w) n_{fs} \cdot (v \cdot n_{fs}) n_{fs} dx + \int_{\Sigma_{c}} \mathbf{T}(w) n_{fs} \cdot P_{\tau}v dx
- \int_{\Sigma_{c}} (v \cdot n_{fs}) Q dx + \int_{\Sigma_{c}} (v \cdot n_{fs}) \psi + \int_{\Sigma_{c}} \frac{\kappa}{\mu} (\nabla \psi \cdot n_{fs}) z dx = 0,$$

which follows

$$\int_{\Sigma_{c}} z(w \cdot n_{fs}) dx + \int_{\Sigma_{c}} \frac{\kappa}{\mu} (\nabla \psi \cdot n_{fs}) z dx = 0, \quad \forall \ z \in H^{1}(\Omega_{s}),$$
or $w \cdot n_{fs} + \frac{\kappa}{\mu} \nabla \phi \cdot n_{fs} = 0$ on Σ_{c} (A.19)

and

$$\int_{\Sigma_{c}} (n_{fs} \cdot \mathbf{T}(w) n_{fs} - Q - \psi) \cdot (v \cdot n_{fs}) dx = 0, \quad \forall \ v \in V_{0}^{1}(\Omega_{f}),$$
or $Q - n_{fs} \cdot \mathbf{T}(w) n_{fs} = -\psi$ on Σ_{c} . (A.20)

Furthermore, let

$$\rho \int_{\Sigma_{c}} (u \wedge w) \cdot (P_{\tau}v) dx + \int_{\Sigma_{c}} \frac{\beta \mu}{\sqrt{\kappa}} (P_{\tau}v) \cdot (P_{\tau}w) dx + \int_{\Sigma_{c}} (\mathbf{T}(w) n_{\mathrm{fs}}) \cdot (P_{\tau}v) dx = 0,$$

for any $v \in V_0^1(\Omega_f)$, where

$$\int_{\Sigma_{c}} (\mathbf{T}(w)n_{fs}) \cdot (P_{\tau}v) dx = \int_{\Sigma_{c}} (P_{\tau}(\mathbf{T}(w)n_{fs})) \cdot (P_{\tau}v) dx.$$

Then we have

$$-P_{\tau}(\mathbf{T}(w)n_{\mathrm{fs}}) - \frac{\beta\mu}{\sqrt{\kappa}}P_{\tau}w = \rho(u \wedge w) \quad \text{on } \Sigma_{\mathrm{c}}. \tag{A.21}$$

In summary, equations (A.12)–(A.21) form the adjoint system (5.39)–(5.48).

On the other hand, note that adding (A.10) with (A.11) and using the boundary conditions (A.15)–(A.21) yield

$$0 = \rho(v, (\nabla u)^{\mathrm{T}} w)_{\Omega_{\mathrm{f}}} - \rho(v, u \cdot \nabla w)_{\Omega_{\mathrm{f}}} + (v, \nabla Q - \nabla \cdot (\mu(\nabla w + (\nabla w)^{\mathrm{T}}))_{\Omega_{\mathrm{f}}} + \int_{\Sigma_{\mathrm{c}}} \left(-\frac{\beta \mu}{2\kappa^{3/2}} h \right) (P_{\tau} u) \cdot (P_{\tau} w) \mathrm{d}x + \left(\frac{1}{\mu} h \nabla \phi, \nabla \psi \right)_{\Omega_{\mathrm{s}}} - \left(z, \nabla \cdot \left(\frac{\kappa}{\mu} \nabla \psi \right) \right)_{\Omega_{\mathrm{s}}}.$$
(A.22)

Finally, with the help of (A.12) and (A.14) we obtain

$$\begin{aligned}
\left(v, \mathcal{C}^*(\mathcal{C}u - \vec{y}_{ref})\right)_{\Omega_f} &= \left(v, \rho((\nabla u)^T w - u \cdot \nabla w)\right)_{\Omega_f} \\
&+ \left(v, \nabla Q - \nabla \cdot \left(\mu(\nabla w + (\nabla w)^T)\right)_{\Omega_f} \\
&= \int_{\Sigma_c} \frac{\beta \mu}{2\kappa^{3/2}} h(P_\tau u) \cdot (P_\tau w) dx - \left(\frac{1}{\mu} h \nabla \phi, \nabla \psi\right)_{\Omega_s}.
\end{aligned} \tag{A.23}$$

ORCID iDs

Sepideh Afshar https://orcid.org/0000-0001-8778-4386 Weiwei Hu https://orcid.org/0000-0002-4752-0893

References

- Abergel F and Temam R 1990 On some control problems in fluid mechanics *Theor. Comput. Fluid Dyn.* 1 303–25
- [2] Adrian R J 2005 Twenty years of particle image velocimetry Exp. Fluids 39 159-69
- [3] Alhammadi A M, Gao Y, Akai T, Blunt M J and Bijeljic B 2020 Pore-scale x-ray imaging with measurement of relative permeability, capillary pressure and oil recovery in a mixed-wet microporous carbonate reservoir rock Fuel 268 117018
- [4] Azzam M I S and Dullien F A L 1976 Calculation of the permeability of porous media from the Navier–Stokes equation Ind. Eng. Chem. Fund. 15 281–5
- [5] Badia S, Quaini A and Quarteroni A 2009 Coupling Biot and Navier-Stokes equations for modelling fluid-poroelastic media interaction *J. Comput. Phys.* 228 7986–8014
- [6] Banks H T and Kunisch K 2012 Estimation Techniques for Distributed Parameter Systems (Boston: Birkhauser)
- [7] Baychev T G, Jivkov A P, Rabbani A, Raeini A Q, Xiong Q, Lowe T and Withers P J 2019 Reliability of algorithms interpreting topological and geometric properties of porous media for pore network modelling *Transp. Porous Media* 128 271–301
- [8] Bear J 2013 Dynamics of Fluids in Porous Media (New York: Dover)
- [9] Beavers G S and Joseph D D 1967 Boundary conditions at a naturally permeable wall *J. Fluid Mech.* 30 197–207
- [10] Berdichevsky A L and Cai Z 1993 Preform permeability predictions by self-consistent method and finite element simulation *Polym. Compos.* 14 132–43
- [11] Berg C F 2014 Permeability description by characteristic length, tortuosity, constriction and porosity Transp. Porous Media 103 381–400

- [12] Borcea L 2002 Electrical impedance tomography Inverse Problems 18 R99
- [13] Conca C, Murat F and Pironneau O 1994 The Stokes and Navier–Stokes equations with boundary conditions involving the pressure *Japan. J. Math.* 20 279–318
- [14] Dauge M 1989 Stationary Stokes and Navier-Stokes systems on two- or three-dimensional domains with corners. Part I. Linearized equations SIAM J. Math. Anal. 20 74-97
- [15] Dias M R, Fernandes P R, Guedes J M and Hollister S J 2012 Permeability analysis of scaffolds for bone tissue engineering J. Biomech. 45 938–44
- [16] Emblem K E, Farrar C T, Gerstner E R, Batchelor T T, Borra R J H, Rosen B R, Sorensen A G and Jain R K 2014 Vessel calibre-a potential MRI biomarker of tumour response in clinical trials *Nat. Rev. Clin. Oncol.* 11 566
- [17] Fairweather J D, Cheung P, St-Pierre J and Schwartz D T 2007 A microfluidic approach for measuring capillary pressure in PEMFC gas diffusion layers *Electrochem. Commun.* 9 2340-5
- [18] Galindo-Rosales F J, Campo-Deaño L, Pinho F T, Van Bokhorst E, Hamersma P J, Oliveira M S N and Alves M A 2012 Microfluidic systems for the analysis of viscoelastic fluid flow phenomena in porous media *Microfluid. Nanofluid.* 12 485–98
- [19] Gao Y, Lin Q, Bijeljic B and Blunt M J 2017 X-ray microtomography of intermittency in multiphase flow at steady state using a differential imaging method *Water Resour. Res.* 53 10274–92
- [20] Girault V and Raviart P-A 2012 Finite Element Methods for Navier-Stokes Equations: Theory and Algorithms vol 5 (Berlin: Springer)
- [21] Glowinski R and Pironneau O 1992 Finite element methods for Navier–Stokes equations *Annu. Rev. Fluid Mech.* **24** 167–204
- [22] Guan K M, Nazarova M, Guo B, Tchelepi H, Kovscek A R and Creux P 2019 Effects of image resolution on sandstone porosity and permeability as obtained from x-ray microscopy *Transp. Porous Media* 127 233–45
- [23] Hasanov A and Baysal O 2016 Identification of unknown temporal and spatial load distributions in a vibrating Euler–Bernoulli beam from Dirichlet boundary measured data *Automatica* 71 106–17
- [24] Hinze M, Kaltenbacher B and Quyen T N T 2018 Identifying conductivity in electrical impedance tomography with total variation regularization *Numer. Math.* 138 723–65
- [25] Hinze M, Pinnau R, Ulbrich M and Ulbrich S 2008 Optimization with PDE Constraints vol 23 (Netherlands: Springer)
- [26] Jain R K 1994 Barriers to drug delivery in solid tumors Sci. Am. 271 58-65
- [27] Jang S H, Wientjes M G, Lu D and Au J L S 2003 Drug delivery and transport to solid tumors Pharm. Res. 20 1337–50
- [28] Jivkov A P, Hollis C, Etiese F, McDonald S A and Withers P J 2013 A novel architecture for pore network modelling with applications to permeability of porous media J. Hydrol. 486 246–58
- [29] Jouini M S, AlSumaiti A, Tembely M, Hjouj F and Rahimov K 2020 Permeability upscaling in complex carbonate samples using textures of micro-computed tomography images *Int. J. Modelling Simul.* 40 245–59
- [30] Kamran N N, Drakunov S V and Solano W M 2017 Nonlinear observer for distributed parameter systems described by decoupled advection equations J. Vib. Control 23 1152–65
- [31] Kamrava S, Tahmasebi P and Sahimi M 2020 Linking morphology of porous media to their macroscopic permeability by deep learning *Transp. Porous Media* 131 427–48
- [32] Kawano A 2014 Uniqueness in the identification of asynchronous sources and damage in vibrating beams *Inverse Problems* 30 065008
- [33] Khawar I A, Kim J H and Kuh H-J 2015 Improving drug delivery to solid tumors: priming the tumor microenvironment J. Control. Release 201 78–89
- [34] Kohn R and Vogelius M 1984 Determining conductivity by boundary measurements Commun. Pure Appl. Math. 37 289–98
- [35] Kohn R V and Vogelius M 1985 Determining conductivity by boundary measurements ii. interior results Commun. Pure Appl. Math. 38 643–67
- [36] Kohn R V and Vogelius M 1987 Relaxation of a variational method for impedance computed tomography Commun. Pure Appl. Math. 40 745–77
- [37] Kubo T, Matsuda N, Kashiwaya K, Koike K, Ishibashi M, Tsuruta T, Matsuoka T, Sasao E and Lanyon G W 2019 Characterizing the permeability of drillhole core samples of toki granite, central Japan to identify factors influencing rock-matrix permeability Eng. Geol. 259 105163
- [38] Kunisch K and Peichl G 1991 Estimation of a temporally and spatially varying diffusion coefficient in a parabolic system by an augmented Lagrangian technique *Numer. Math.* 59 473–509

- [39] Landa-Marbán D, Liu N, Pop I S, Kumar K, Pettersson P, Bødtker G, Skauge T and Radu F A 2019 A pore-scale model for permeable biofilm: numerical simulations and laboratory experiments *Transp. Porous Media* 127 643–60
- [40] Lions J L 1971 Optimal control of systems governed by partial differential equations problèmes aux limites
- [41] Lions J L and Magenes E 2012 Non-Homogeneous Boundary Value Problems and Applications: Volume 1 vol 181 (Berlin: Springer)
- [42] Mahammod B P, Barua E, Deoghare A B and Pandey K M 2020 Permeability quantification of porous polymer scaffold for bone tissue engineering *Mater. Today* 22 1687–93
- [43] Maz'ya V and Rossmann J 2009 Mixed boundary value problems for the stationary Navier–Stokes system in polyhedral domains Arch. Ration. Mech. Anal. 194 669–712
- [44] Mochi M, Pacelli G, Recchioni M C and Zirilli F 1999 Inverse problem for a class of twodimensional diffusion equations with piecewise constant coefficients J. Optim. Theory Appl. 100 29-57
- [45] Moura S, Bendtsen J and Ruiz V 2014 Parameter identification of aggregated thermostatically controlled loads for smart grids using PDE techniques Int. J. Control 87 1373–86
- [46] Mueller J L and Siltanen S 2012 Linear and Nonlinear Inverse Problems with Practical Applications (Philadelphia, PA: SIAM)
- [47] Nel A, Ruoslahti E and Meng H 2017 New insights into permeability as in the enhanced permeability and retention effect of cancer nanotherapeutics
- [48] Nguyen P A and Raymond J-P 2015 Boundary stabilization of the Navier-Stokes equations in the case of mixed boundary conditions SIAM J. Control Optim. 53 3006-39
- [49] Nguyen V T, Georges D and Besançon G 2016 State and parameter estimation in 1-d hyperbolic pdes based on an adjoint method Automatica 67 185–91
- [50] Nocedal J and Wright S 2006 Numerical Optimization (New York: Springer)
- [51] Okabe H and Blunt M J 2004 Prediction of permeability for porous media reconstructed using multiple-point statistics *Phys. Rev.* E 70 066135
- [52] Ooi E H and Ooi E T 2017 Mass transport in biological tissues: comparisons between singleand dual-porosity models in the context of saline-infused radiofrequency ablation Appl. Math. Modelling 41 271–84
- [53] Ovaysi S and Piri M 2010 Direct pore-level modeling of incompressible fluid flow in porous media J. Comput. Phys. 229 7456–76
- [54] Pennella F, Cerino G, Massai D, Gallo D, Labate G F D, Schiavi A, Deriu M A, Audenino A and Morbiducci U 2013 A survey of methods for the evaluation of tissue engineering scaffold permeability Ann. Biomed. Eng. 41 2027–41
- [55] Perrault S D, Walkey C, Jennings T, Fischer H C and Chan W C W 2009 Mediating tumor targeting efficiency of nanoparticles through design *Nano Lett.* 9 1909–15
- [56] Picchi D and Battiato I 2019 Relative permeability scaling from pore-scale flow regimes Water Resour. Res. 55 3215–33
- [57] Prabhakar U et al 2013 Challenges and key considerations of the enhanced permeability and retention effect for nanomedicine drug delivery in oncology
- [58] Premžoe S, Tasdizen T, Bigler J, Lefohn A and Whitaker R T 2003 Particle-based simulation of fluids Comput. Graph. Forum 22 401–10
- [59] Rezaei Niya S M and Selvadurai A P S 2017 The estimation of permeability of a porous medium with a generalized pore structure by geometry identification *Phys. Fluids* 29 037101
- [60] Santos J, Pires T, Gouveia B P, Castro A P G and Fernandes P R 2020 On the permeability of TPMS scaffolds J. Mech. Behav. Biomed. Mater. 110 103932
- [61] Schiavi A, Guglielmone C, Pennella F and Morbiducci U 2012 Acoustic method for permeability measurement of tissue-engineering scaffold Meas. Sci. Technol. 23 105702
- [62] Spall J C 2005 Introduction to Stochastic Search and Optimization: Estimation, Simulation, and Control vol 65 (New York: Wiley)
- [63] Temam R 2001 Navier-Stokes Equations: Theory and Numerical Analysis vol 343 (Providence, RI: American Mathematical Society)
- [64] Tröltzsch F 2010 Optimal Control of Partial Differential Equations: Theory, Methods, and Applications vol 112 (Providence, RI: American Mathematical Society)
- [65] Truscello S, Kerckhofs G, Van Bael S, Pyka G, Schrooten J and Van Oosterwyck H 2012 Prediction of permeability of regular scaffolds for skeletal tissue engineering: a combined computational and experimental study *Acta Biomater.* 8 1648–58

- [66] Uhlmann G 2009 Electrical impedance tomography and Calderón's problem *Inverse Problems* 25 123011
- [67] Wang C, Pan L, Zhao Y, Zhang Y and Shen W 2019 Analysis of the pressure-pulse propagation in rock: a new approach to simultaneously determine permeability, porosity, and adsorption capacity *Rock Mech. Rock Eng.* 52 4301–17
- [68] Wang Y D, Chung T, Armstrong R T, McClure J, Ramstad T and Mostaghimi P 2020 Accelerated computation of relative permeability by coupled morphological and direct multiphase flow simulation J. Comput. Phys. 401 108966
- [69] Westerweel J, Elsinga G E and Adrian R J 2013 Particle image velocimetry for complex and turbulent flows Annu. Rev. Fluid Mech. 45 409–36
- [70] White F M 1999 Fluid Mechanics web edn (New York: McGraw-Hill)
- [71] Wu M, Xiao F, Johnson-Paben R M, Retterer S T, Yin X and Neeves K B 2012 Single- and two-phase flow in microfluidic porous media analogs based on Voronoi tessellation *Lab Chip* 12 253–61
- [72] Wu Z, Yin J and Wang C 2006 Elliptic & Parabolic Equations (Singapore: World Scientific)
- [73] Xiong Q, Baychev T G and Jivkov A P 2016 Review of pore network modelling of porous media: experimental characterisations, network constructions and applications to reactive transport J. Contam. Hydrol. 192 101–17
- [74] Yang S and Gao H 2017 Nanoparticles for modulating tumor microenvironment to improve drug delivery and tumor therapy *Pharmacol. Res.* 126 97–108
- [75] Yang X-S and Zhou B 2002 A new numerical model for Stokes flow and permeability estimation Discrete Element Methods: Numerical Modeling of Discontinua pp 195–9
- [76] Yhee J Y et al 2017 Effects of tumor microenvironments on targeted delivery of glycol chitosan nanoparticles J. Control. Release 267 223–31
- [77] Yu Q, Dai Z, Zhang Z, Soltanian M R and Yin S 2019 Estimation of sandstone permeability with SEM images based on fractal theory *Transp. Porous Media* 126 701–12
- [78] Zhang P et al 2018 Tumor microenvironment-responsive ultrasmall nanodrug generators with enhanced tumor delivery and penetration J. Am. Chem. Soc. 140 14980–9